## Climatic and geomorphologic cycles in a semiarid distributive fluvial system, Upper Cretaceous, Bauru Group, SE Brazil

Marcus Vinícius Theodoro Soares [a], Giorgio Basilici [a,b,e], Patrick Führ Dal' Bó [c,e], Thiago da Silva Marinho [d], Nigel Philip Mountney [e], Luca Colombera [e], Emerson Ferreira de Oliveira [a], Karla Evenny Brito da Silva [a]

[a] Department of Geology and Natural Resources, Institute of Geosciences, State University of Campinas, 13083-870, Campinas, SP, Brazil
[b] Centro Regional de Investigaciones Científicas y Transferencia Tecnológica/CONICET, Argentina
[c] Department of Geology, Institute of Geosciences, Federal University of Rio de Janeiro, Rio de Janeiro, RJ, Brazil
[d] Centro de Pesquisas Paleontológicas L. I. Price, CCCP/UFTM, 38001-970, BR-262, Km 784, Peirópolis, Uberaba, MG, Brazil
[e] Fluvial & Eolian Research Group, School of Earth and Environment, University of Leeds, Leeds LS2 9JT, UK

**ABSTRACT**
Studies of distributive fluvial systems and their preserved successions envisage the distribution and orientation of architectural elements to be primarily controlled by channels radiating outward from fan apices, in many cases along an elongate basin margin. Conceptual models for such systems account for the downstream dynamics of the fluvial network, but with limited consideration of temporal geomorphic variations, resulting vertical organisation of architectural elements, or of the interplay of factors controlling system dynamics. To understand the external and internal architecture of distributive fluvial systems, and the factors that influence their sequential facies organisation, a sedimentary succession of the proximal portion of an Upper Cretaceous, semiarid, distributive fluvial system, located at the north-eastern margin of the Bauru Basin (Southeast Brazil), has been analysed in detail. Three fining- and thinning-upward fluvial sequences are identified, forming an interval separated at the top and the bottom by two palaeosol profiles. Each sequence is formed of channel and floodplain deposits. Two types of channel deposits are identified. One is composed of stacked sets of small-scale dune deposits, suggesting perennial and steady fluvial regime, associated with more humid climate periods. The other is composed of large-scale sets indicative of flattened dunes associated with unsteady and fast-changing fluvial flow, formed in quasi-supercritical flow regime conditions, associated with drier climate periods. The vertical alternation of these two types of channel deposits records the accumulation of a fluvial succession that responded to high-frequency, climate-induced cyclic change in bounding conditions. Two palaeosol profiles, at the top and at the bottom of the succession, indicate temporary interruptions and cessation of the fluvial sedimentation, likely related to avulsion of the fluvial belt. Thus, the studied succession reveals high-frequency climate-induced allogenic sedimentary cycles that occur within a long-period autogenic geomorphologic-induced sedimentary cycle. This work suggests that the internal architecture of the channel deposits can be used as a climate proxy, and that climate and geomorphology act jointly as notable factors to control the vertical organisation of distributive fluvial systems.
**Keywords:** Fluvial deposits; Palaeohydrology; Semiarid climate; Bauru Basin; Upper Cretaceous.

### 1. INTRODUCTION
Facies models describing the arrangement of deposits of many fluvial systems and their preserved successions derive largely from studies of modern tributary rivers developed in humid climatic settings

(e.g., Miall, 1996; Bridge, 2006). A perceived bias in the choice of modern fluvial systems used to develop such facies models has increasingly been questioned in recent years, and is highlighted by the recognition that much of the fill of actively developing modern continental sedimentary basins is composed of the accumulated deposits of distributive fluvial systems (Weissmann et al., 2010). Moreover, deposits of dryland rivers might have been underrepresented in fluvial sedimentology literature (Fielding et al., 2009). In fact, the highly variable hydraulic behaviour typically associated with dryland rivers is equally observed in a broad range of climatic settings in the seasonal tropics and even in more humid settings in the subtropics (Fielding et al., 2009). Consequently, prevailing facies models based primarily on tributary and humid fluvial systems are not necessarily suitable tools for understanding the large range of facies architectures documented from the rock record, in particular those suggested to be indicative of dryland distributive fluvial systems (Fielding et al., 2009; Weissmann et al., 2010).

Modern dryland fluvial systems have been studied in the arid and semiarid regions of Australia (Tooth, 1999), Israel (Schick, 1993) and South Africa (Tooth and Nanson, 1995), as well as other places. These studies prioritize the characterization of dryland fluvial environments according to their hydraulic behaviour, which is controlled by a highly variable rainfall in both time and space (Tooth, 2000). Flows normally occur as high-energy flash floods, triggered by rainfall episodes with isolated, multiple or seasonal peaks (Graf, 1988). Although most dryland rivers are typified by ephemeral channel flow related to episodic puloses of discharge, it is possible for these rivers to assume an intermittent or even perennial discharge regime, when associated with episodes of seasonal rainfall (Tooth, 2000) or where catchments are sourced in adjacent highland areas with greater precipitation than the downstream receiving basin.

Due to the absence or scarcity of vegetation, dryland basins tend to yield a substantial volume of sediment that is susceptible to remobilization during flood events. The absence of a widespread vegetation cover that would otherwise dampen runoff tends to result in floods characterised by markedly peaked hydrographs. Such flood events commonly have substantial erosive power (Plink-Björklund, 2015). This scenario forces the channels to constantly readapt to new hydraulic conditions (nonequilibrium), resulting in the development of rivers that are highly sensitive in geomorphologic terms (Tooth, 2000).

In the rock record, deposits of ancient dryland fluvial systems reveal distinct characteristics. Their architecture commonly reveals channel bodies with complex vertical and lateral arrangement of sedimentary facies (McKie, 2011). As a consequence of their highly energetic and variable discharge, dryland rivers commonly preserve sedimentary structures formed in upper-stage plane-bed conditions and lack macroform elements that are typical in deposits of perennial rivers (Fielding et al., 1999). Successive variations in the hydraulic regime of dryland rivers are preserved in the geologic record as channelised bodies of different architecture (Colombera et al., 2012, 2013). Consequently, channel bodies provide excellent palaeoclimatic proxies for reconstructing ancient fluvial systems.

Conceptual models of dryland distributive fluvial systems are based on rivers whose dynamics reveal a clear downstream reduction in water discharge from proximal to distal zones. Between these zones it is possible to observe a decrease in channel dimension and grain size, and an increase in non-channelised flows, commonly culminating in development of terminal splay complexes (Parkash et al., 1983; Abdullatif, 1989; Nichols and Fisher, 2007). Many such systems (both modern and ancient) are divided in three zones (proximal, intermediate and distal) based on downstream changes of the architectural elements (Cain and Mountney, 2009, see their Fig. 1). Downstream, dryland fluvial systems may pass to a playa-lake, to a permanent water body, to a larger fluvial system, to an aeolian sand sea or to a sand sheet (Almasrahy and Mountney, 2015), or to a marine shoreline, depending on the regional geography and climate.

In the geological record, the recognition of dryland distributive fluvial systems is based on the characteristics of the facies that indicate downstream decrease in hydraulic discharge, channels dimension, channelised flows, and an increase of non-channelised flows (sheet-like flows), channel bifurcation and occurrence of aeolian, playa-lake, coastal, wetland or lacustrine deposits (e.g., Nichols and Fischer, 2007; Cain and Mountney, 2009). Many models for these types of system have been developed from studies of endorheic basins in arid to semiarid climate conditions (e.g., Nichols and Fisher, 2007). Our current understanding of dryland distributive fluvial systems relies primarily on the recognition of arrangement (e.g., lateral distribution and orientation) of architectural elements, controlled by the outward radiation of channels from a fan apex. This conceptual framework accounts for the lateral variation of facies and architecture of the fluvial network, but gives only limited consideration to temporal variations, vertical organisation of the architectural elements, and to factors that control vertical accumulation. In this regard, the north-eastern margin of the Bauru Basin (Upper Cretaceous, southeast Brazil), which hosts excellent exposures of deposits related to a semiarid distributive fluvial system (Basilici et al., 2016a), offers ideal conditions for a detailed study on the vertical stratigraphic organisation of dryland distributive fluvial succession and an assessment of controls that acted upon the formative system.

The aim of this paper is to understand the key mechanisms controlling the dynamics of a dryland distributive fluvial system and assess how they determine the high-frequency stratigraphic organisation of these systems in the geologic record. Specific research objectives are as follows: (i) to show how accumulated channelised bodies can be interpreted as palaeoclimatic proxies; and (ii) to describe how arrangements of lithofacies and architectural elements of dryland distributive fluvial systems can help determine what factors govern the dynamics and the temporal variations in the style of accumulation of distributive fluvial systems.

## 2. GEOLOGICAL AND STRATIGRAPHIC SETTING

### 2.1. The Bauru Basin

The Bauru Basin is an endorheic sag basin whose origin and evolution range from Coniacian to Maastrichian, according to biostratigraphic considerations (Dias-Brito et al., 2001) and based on radiometric dating from igneous intrusions bordering the limits of the basin (Coutinho et al., 1982). The Bauru Basin developed under the “Hot and Arid Southern Belt Zone” (Chumakov, 1995) and it hosted one of the most extensive dryland environments of the Cretaceous period, occupying an area of *c.*370,000 $km^2$ (Fig. 1A). The sedimentation of the Bauru Basin started in the aftermath of the continental break-up of South America and Africa, when the opening of the Proto-Atlantic Ocean established one the largest basalt effusions recorded on the Earth's history, the Paraná-Etendeka Continental Flood Basalt Province (Milani et al., 2007).

The Bauru Basin is composed of *c.*450 m-thick siliciclastic succession that overlays the flood basalts. The succession is subdivided in two groups: the Caiuá and Bauru Groups. The study succession examined here belongs to the Bauru Group, which is subdivided into the Araçatuba Formation (playa-lake systems), Adamantina Formation (alluvial systems) and Marília Formation (alluvial system) (Fig. 1C). The Marília Formation constitutes the upper portion of the Bauru Basin. This unit developed during the Upper Cretaceous (Dias-Brito et al., 2001) and is represented by a 160-m thick succession, primarily composed of chemically immature, poorly-sorted, coarse- to fine-grained sandstone, and secondarily of conglomerate and mudstone deposits.

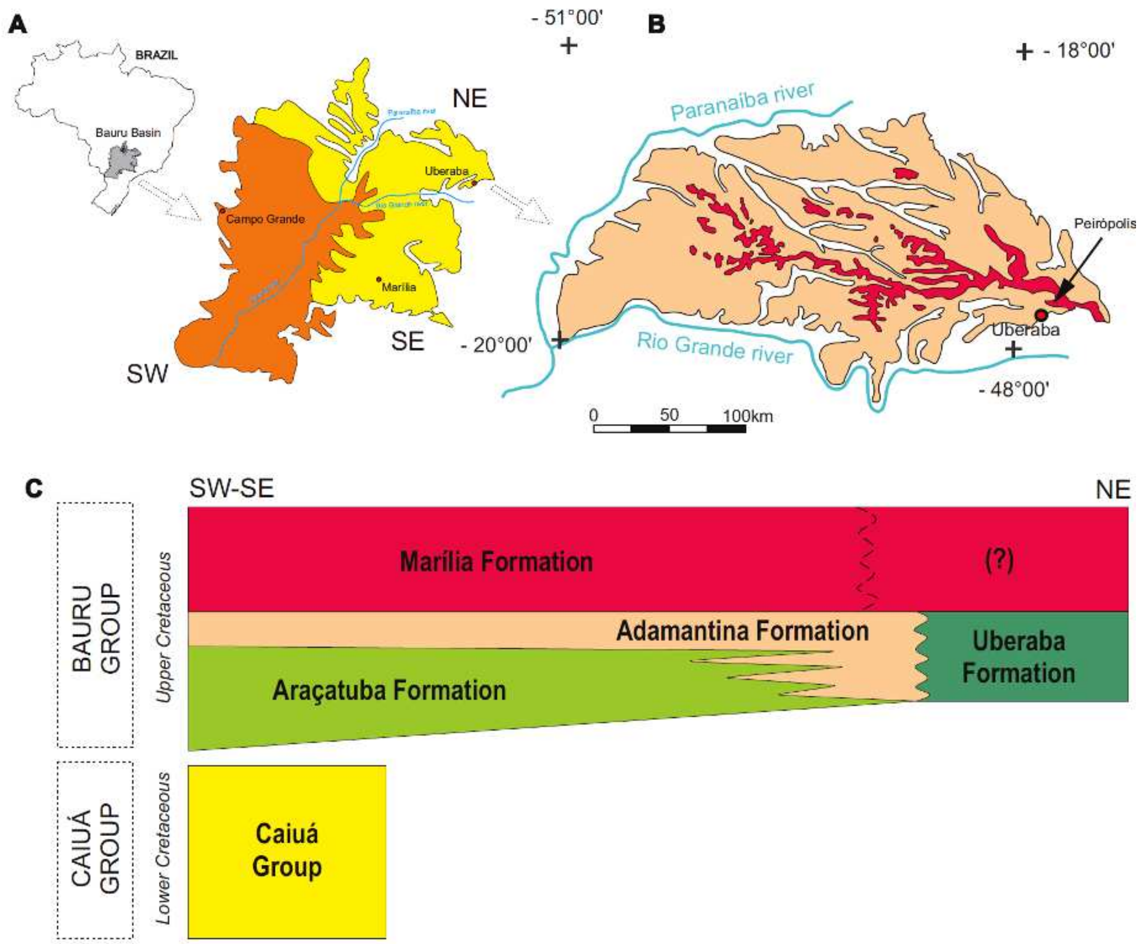


**Figure 1.** (A) Location map and lithostratigraphic map of the Bauru Basin. (B) Lithostratigraphic map of the northeastern sector of the Bauru Basin (Minas Gerais State) with detail to the study area (Peirópolis) near the city of Uberaba; (C) Lithostratigraphy of the Bauru Basin (modified from Basilici et al.,2016). The lithostratigraphic map was modified from the Geological Survey of Brazil (CPRM, 2004).

## 2.2. Study area

The study area is located at the northern part of the Bauru Basin near the town of Peirópolis (Fig. 1B), where the Marília Formation has been mapped (CPRM - Geological Survey of Brazil, 2004). However, the lithostratigraphic features of the studied succession differ markedly from those in the description of the type section of the Marília Formation at the south-central part of the basin (Soares et al., 1980). Contrasting opinions on the lithostratigraphic nature of this unit are discussed in literature (Basilici et al., 2016b). For these reasons, and in the absence of a clearer lithostratigraphic definition, we herein refer to the succession studied here as the upper portion of the Bauru Group.

The study area (Peirópolis, Fig. 2A) is considered the proximal portion of a distributive fluvial system. To demonstrate this hypothesis, biostratigraphic data, architectural features, petrographic composition and palaeocurrent data were employed to compare the sedimentary succession exposed in the study area with another excellent exposure of the same unit located *c.* 35 km toward NE (BR50, Fig. 2A), and interpreted as the medial portion of the same fluvial system. Four important observations are made. First, the palaeontological remains discovered in both these sites belong to amiid fishes, podocnemidoid turtles, peirosaurid crocodyliforms, abelisaurid theropods and titanosaur sauropods (Novas et al., 2008; Martinelli et al., 2013; Martinelli and Teixeira, 2015). The fossil assemblage comprises the same species, which demonstrates that both sites are contemporaneous and represent a corresponding palaeoecological system. Second, the site of Peirópolis is characterised by sheet-like amalgamated channel elements, with only scarce floodplain deposits. By contrast, the site of BR50 is characterised sheet and ribbon channels separated by thick floodplain deposits (Fig. 2B). The ratio channel-to-floodplain deposits (measured in terms of thickness) varies from 7.9 to 2.5 from Peirópolis to the BR50 site. This architectural organisation is analogous to observations made for other distributive fluvial systems (e.g., Nichols and Fisher, 2007; Cain and Mountney, 2009). Third, the petrographic composition at both sites (Fig. 2C) displays similar mineralogical composition, defining the same provenance area and suggesting that they are part of the same fluvial system. Fourth, palaeocurrent indicators, measured from sedimentary structures in channel deposits, indicate consistent palaeoflow direction toward the northeast, supporting the hypothesis that the channel deposits belonged to the same fluvial system (Fig. 2D). According to these data, we suggest that both sites are part of the same fluvial distributive palaeoenvironment in which the Peirópolis study area and the BR050 site correspond to a more proximal and intermediate portions of the system, respectively.

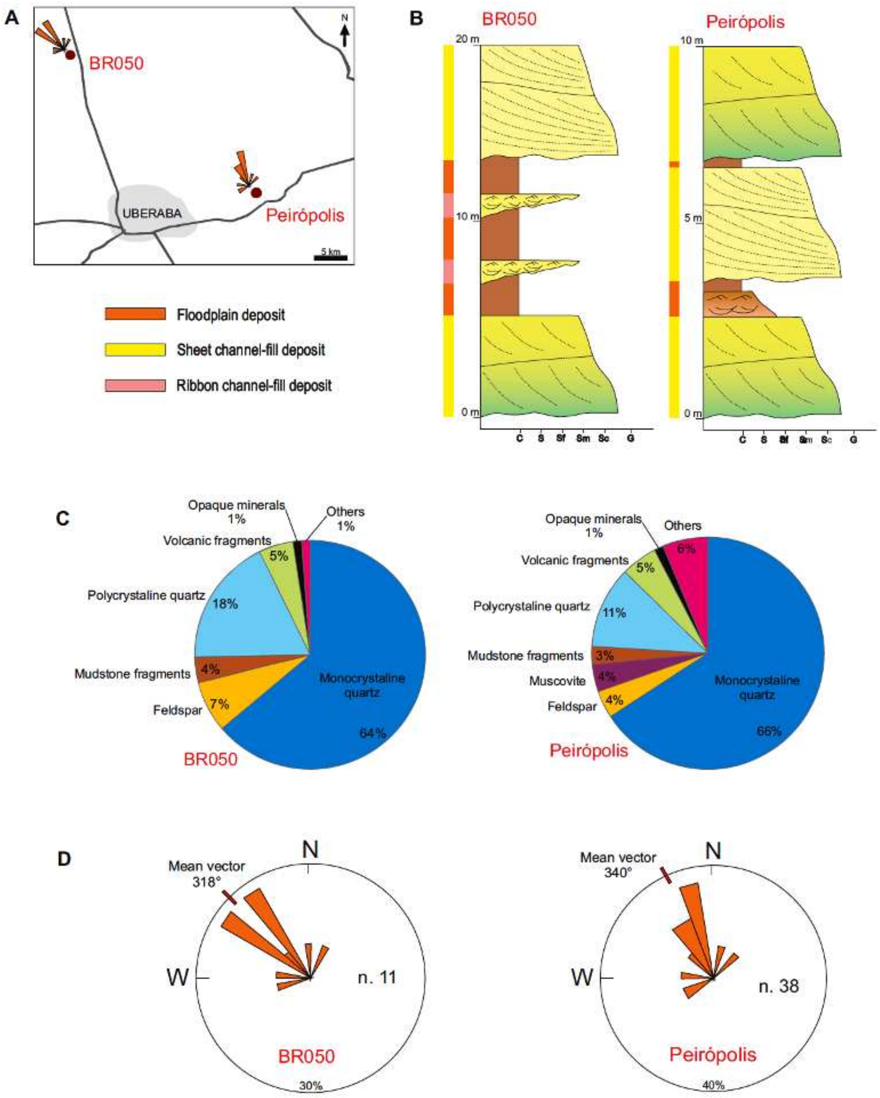


**Figure 2.** Stratigraphic correlation between the Peirópolis and the BR050 sites as proximal and intermediate parts of a distributive fluvial system, respectively. Figure (A) shows their relative location and mean palaeocurrent. Correlation between the Peirópolis and BR050 sites is demonstrated by comparing their: (B) stratigraphic sections, (C) petrographic composition and (D) palaeocurrent data.

## 3. METHODS

An abandoned quarry located near the town of Peirópolis (Fig. 2A) allowed a detailed study of the sedimentary succession. The quarry provides excellent exposures that reveal the three-dimensional nature of the succession. Five detailed stratigraphic sections, each *c.*10 m thick, were measured and analysed at centimetre resolution. Thirty-four other outcrops, plus another excellent exposure at site BR50 (Fig. 2A), were analysed from a total area of 450 km$^2$ around the study site. Data from these sites were used to better define the sedimentological features that constitute the studied interval and define the proximal position of the depositional system. Fluvial deposits were subdivided into nine lithofacies, each with identifiable genetic significance (*sensu* Harms et al., 1982), based on grain size, sorting, fabric, mineralogy, beds thickness, geometry, bounding surfaces, sedimentary structures, palaeocurrent indicators and type (if any) of bioturbation (Tab 1). Palaeosols were recognised in the field by the presence of destratification, root marks, nodules, mottles, colour patterns and bioturbation (Retallack, 1988; Catt, 1990). The arrangement of lithofacies has been considered by tracing the boundaries and sequential organisation of containing units and this method has been employed to reconstruct the depositional environment of the studied succession. Three sedimentary sequences, each comprising channel-fill and floodplain deposits, have been identified. Within these, facies arrangements have been further assigned to four types of architectural element. The architectural elements were reconstructed through the identification of the commonly occurring lithofacies associations and vertical successions, and by the identification of a hierarchical set of bounding-surface types based on the method of Miall (2006).

## 4. SEQUENTIAL ORGANISATION OF THE STUDY SUCCESSION

The sedimentary succession is delimited below its base and at its top by palaeosol profiles that are 1.25 m and 0.3 m thick, respectively (Fig. 3). Between these palaeosol units, the succession records three depositional bodies, which are separated by erosional surfaces. Each body is characterised by a fining- and thinning-upward succession, 1.6 to 2.35 m thick, and comprising a lower portion of pebbly sandstone or sandstone, and an upper portion of very fine-grained sandstone or mudstone (Fig. 3). The two portions in each body may be identified as channel-fill and floodplain deposits, respectively (see below). Description and interpretation of nine lithofacies and four architectural elements are reported in Table 1 and 2, respectively. Palaeosols are considered in the depositional analysis because they indicate important episodes of cessation of sedimentation and serve as palaeoclimatic proxies.

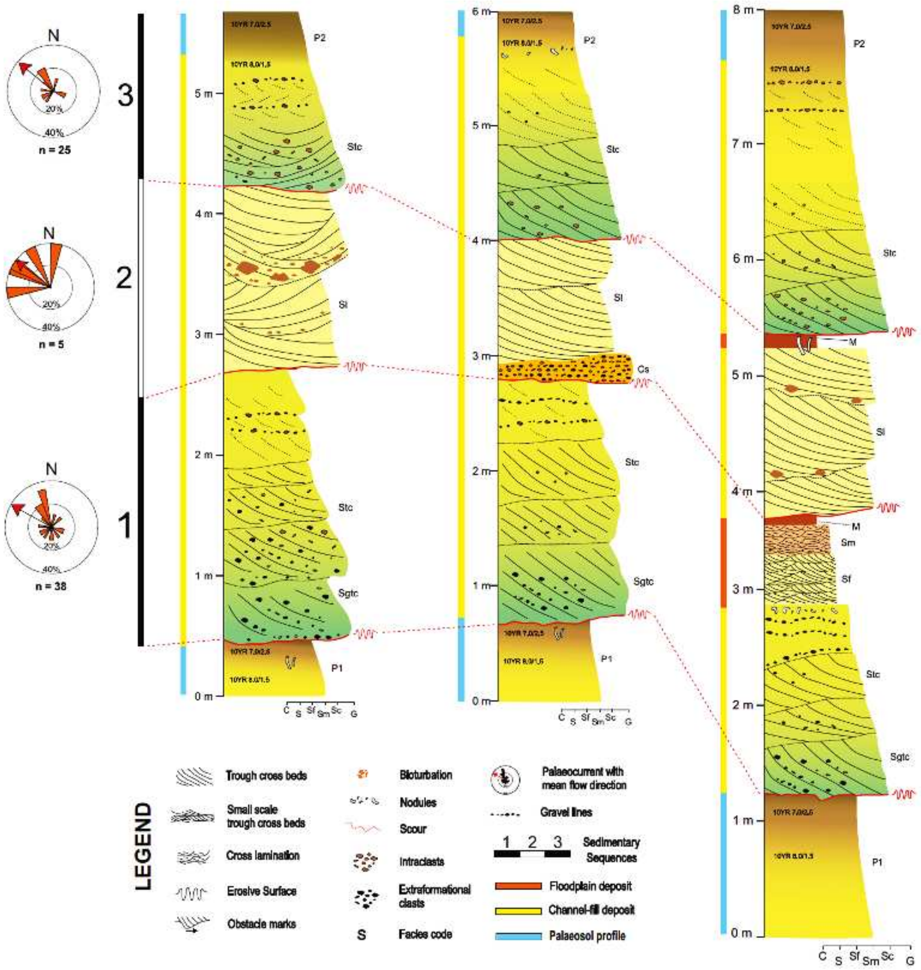


**Figure 3.** Stratigraphic sections of the studied succession. Three sequences of channel-fill deposits overlain by floodplain deposits are indicated with numbers 1 to 3. Palaeosol profiles bounding the fluvial sequences are localised at the base (P1) and top (P2).

### 4.1. FIRST SEQUENCE

The first sequence overlies a palaeosol profile and is composed by 2.3 m-thick, laterally extensive (more than 110 m), sheet-like unit, marked at the bottom by an erosive surface, locally displaying asymmetrical, concave-up shape (0.3 m in vertical relief and 0.5 m wide) scours (Palaeosol architectural element P, Fig. 4A).

The palaeosol profile (lithofacies P1) is 1.25 m thick and laterally continuous below the bottom of the sequence. The top of the profile is marked by an erosional surface, whereas the bottom shows diffuse transition to underlying pebbly sandstone. The grain size records a fining-upward trend from coarse-grained sandstone to medium-grained sandstone. The sandstone clasts are composed of quartz, feldspar and lithic fragments (quartzite, chalcedony and gneiss). The colour varies gradually from reddish pink (10YR 7.0/2.5) at the top to light pink (10YR 8.0/1.5) at the bottom of the profile (Fig. 4B). Bioturbation is present at the top of the profile and is characterised by vertical to sub-vertical tubes showing circular sections up to 8 mm in diameter.

The colour intensification towards the top of the profile indicates rubification, caused by oxidation of the parent material near the palaeosurface (Fenwick, 1985). Bioturbation and rubification indicate exposure to the atmosphere. The absence of horizons relates to an incipient palaeopedogenesis.

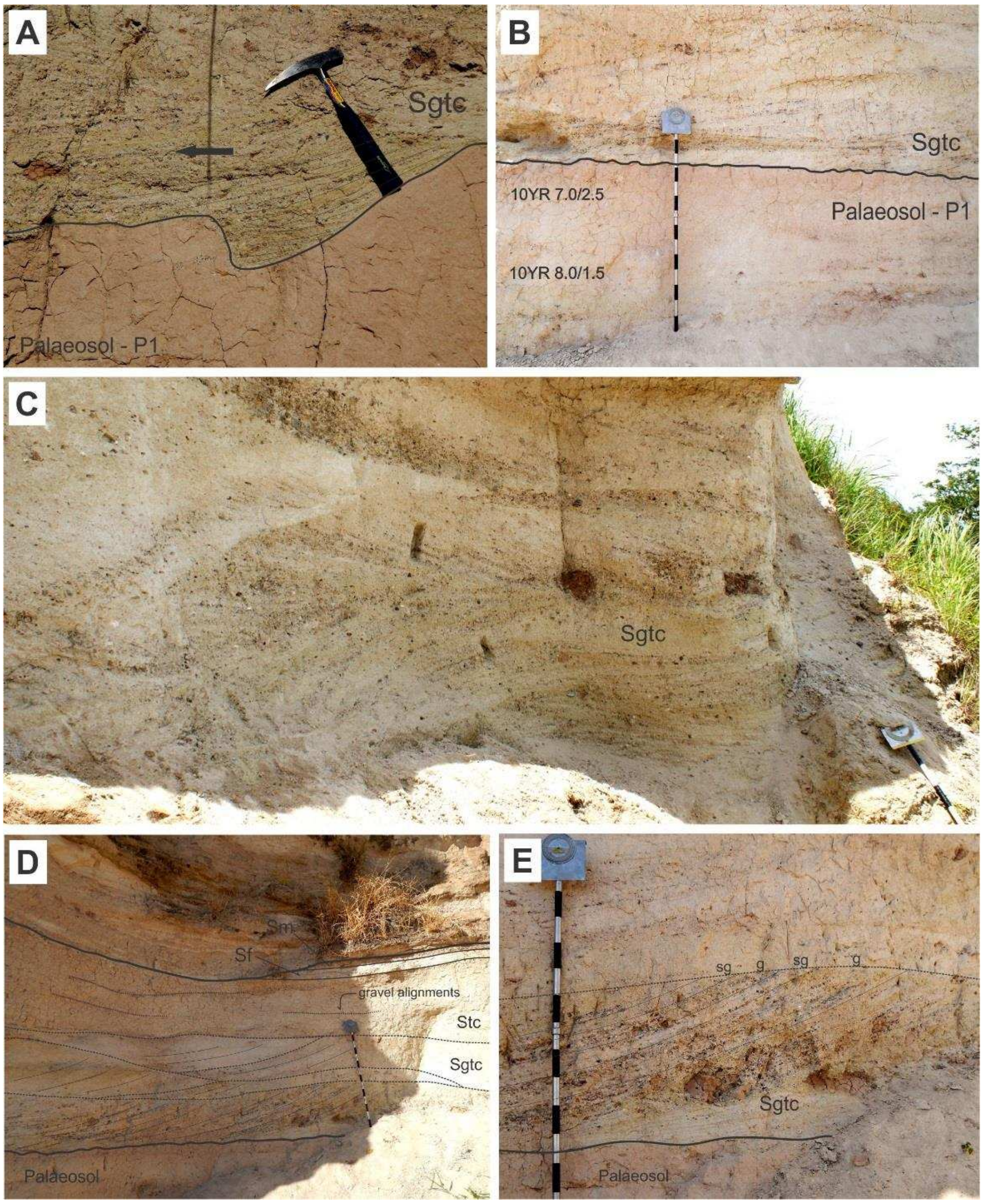


**Figure 4.** First sequence. Palaeosol profiles bounding the first sequence at the base showing (A) asymmetrical, concave-up shape scours and (B) gradual vertical colour variation from reddish pink (10YR 7.0/2.5) at the top to light pink (10YR 8.0/1.5) at the base. (C) Trough cross-bedded pebbly sandstone (lithofacies Sgtc) at the bottom of the first sequence. (D) Gradual vertical transition between the lower (Stgc) and upper portions (Stc) of the first sequence. (E) Cross-stratifications of lithofacies Sgtc showing alternating gravel and coarse- to medium-grained sandstone. Jacob stick is with scale marked by intervals of 10 cm.

#### 4.1.1. Channel-fill deposits

*Description.* Channel-fill deposits are composed of sandstone beds showing fining-upward trend, associated with upward increase in sorting (Fining-up cross-bedded channel CF, Tab. 2). The architectural element (CF) that constitutes these deposits is divided in two lithofacies: trough cross-bedded pebbly sandstone (Sgtc) and trough cross-bedded sandstone (Stc) (Fig. 5, 6 and 7). The trough cross-bedded pebbly sandstone (Sgtc – Tab. 1) is located in the lowermost portion and comprises pebbly sandstone, organised in trough cross-bedded sets, 0.2 to 0.6 m thick and 0.2 to 3 m wide (Fig. 4C, D). Trough axes record uniform modal palaeocurrent direction toward northwest (Fig.

3). Each trough cross-bedded set displays normal grading, evidenced by accumulation at the bottom of granule and cobble clasts of both extraformational and intraformational origin. Extraformational clasts are rounded to well-rounded, and are composed of quartzite, chalcedony and gneiss; intraformational clasts are sub-rounded to angular, and are composed of mudstone and pedogenic calcareous nodules. The foresets of the cross stratifications are angular at their point of intersection with the base of the set in which they occur. Foresets are composed by alternating gravel and coarse- to medium-grained sandstone (Fig. 4E); the sets are bounded at the top by alignments of sandy gravel layers. The upper portion of the channel fill is made of trough cross-bedded sandstone (lithofacies Stc – Tab. 1), which consists of medium-grained sandstone sets, 0.1-0.4 m thick, with indistinct trough cross bedding, made evident only by alignment of granules and small pebbles along the foresets and the set boundaries. The vertical transition between the two portions is gradual (Figs. 4D, 5 and 6).

*Interpretation.* The erosive surface at the bottom of the sequence indicates the transition from a phase of stability and pedogenesis of the topographic surface to a phase of active erosion, transport and deposition of clastic material (Kraus and Wells, 1999). Asymmetrical scours are interpreted as obstacle scours produced by protruding objects (*e.g.* vegetation fragments or large lithoclasts) during initial erosion. The obstacles act as hydrodynamic barriers, locally intensifying the turbulence around them and increasing the erosive power, producing scours at the channel floor (Sanz-Montero et al., 2014). Lenticular beds of trough cross-beddings (lithofacies Sgtc and Stc– Tab. 1) indicate migration and deposition of three-dimensional subaqueous dunes with sinuous crests (Collinson et al., 2006; Miall, 2006). The bimodal sediment distribution along the foresets results from the migration of superimposed bedforms of different grain size and dimensions above the dune stoss side: sandy gravel material is related to smaller bedforms whereas gravel material to larger bedforms (Lunt et al., 2007). The alignment of sandy gravel material at the top of the sets result from difference of mobility between grain size fractions, by an effect referred to as kinetic sorting (Bacchi et al., 2014). During higher discharge, coarser particles are set in motion and temporary voids are created between moving gravel clasts, allowing the downward percolation of finer particles. When discharge decreases, coarser particles cease their movement, producing sandy gravel layers at the top of the dunes (Bacchi et al., 2014). The erosional surface at the bottom of this element and the coarse-grained concave-up geometry of the deposit suggest that this type of element records the filling of a river channel. The overall fining-upward trend of the fill reveals the waning nature of the flow into the channel. The structureless character observed in the uppermost part (lithofacies Stc) relates to the increase in sorting upwards, associated with smaller three-dimensional dunes produced by a low-energy flow. This has likely resulted in the absence of discernable foresets.

| Facies | Code | Lithology | Sedimentary structures | Geometry | Contacts | Interpretation | Figures |
|---|---|---|---|---|---|---|---|
| **Sandy conglomerate** | Cs | Matrix-supported, sandy conglomerate with intraformational and extraformational clasts. Very coarse- to coarse-grained lithoarenite matrix with carbonate cement | Structureless; locally shows crude normal grading | Tabular layers, more than 15 m in lateral extension, and up to 0.5 m thick | Horizontal erosive surfaces at the base and the top | Hyperconcentrated channelised flows | Fig. 9A, B |
| **Trough cross-bedded pebbly sandstone** | Sgtc | Pebbly sandstone with fining-upward trend; extraformational clasts are rounded to well-rounded (quartzite, chalcedony and gneiss); intraformational clasts are sub-rounded to angular (mudstone and pedogenic calcareous nodules) | Trough cross-stratified sets, 0.2 to 0.6 m thick and 0.2 to 3 m wide; sets display normal grading; cross-strata demonstrate alternating gravel and coarse- to medium-grained sandstone | Tabular layers, more than 110 m laterally extended, up to 1.5 m thick | Erosive base overlaid by gravelly deposits and gradual vertical transition at the top with lithofacies Stc. | Three-dimensional subaqueous dunes (sinuous crests) with superimposed smaller bedforms | Fig. 4C, D, E |
| **Trough cross-bedded sandstone** | Stc | Medium-grained sandstone with mudstone intraclasts showing fining-upward trend | Trough cross-stratified sets, 0.1-0.4 m thick, with barely visible trough cross beddings, underlined by alignment of granules and small pebbles along the foresets and the set boundaries | Tabular layers, more than 110 m laterally extended, up to 2 m thick | Gradual vertical transition with lithofacies Sgtc at the base and lithofacies P2 at the top. | Smaller three-dimensional dunes produced by a low-energy flow following deposition of Sgtc | Fig. 4D<br>Fig. 10A, B |
| **Large-scale lenticular cross-bedded sandstone** | Sl | Poorly to moderately sorted, medium to coarse grained sublithoarenite with frequent mudstone intraclasts. | Large-scale lenticular cross-bedded sandstone sets; cross-stratifications have gentle dip (10-15°), concave-up and wedge-shaped, they taper toward the toeset, which is tangential and long. Sets are 10-15 m long (palaeostreamwise) and up to 1.4 m thick | Tabular layers, more than 110 m laterally extended, up to 2 m thick | Base is concave-up; top is planar or mildly concave-up | Large dunes yielded by high-velocity currents, with high amount of suspended materials, at the transition from dune to upper-stage plane-bed fields | Fig. 9C |
| **Fine sandstone** | Sf | Fine-grained sandstone with mudstone | Sets are 0.1 to 0.2 m thick, showing lateral pinch-out and composed of small trough cross-stratifications with dip angles of 15-20° marked by mud drapes; set boundaries are marked mudstone laminae. | c.0.5 m thick layers no more than 25 m in lateral extension | Abrupt transition at the base with lithofacies S and at the top with lithofacies Sm | Small three-dimensional sinuous dunes deposited on the flood plain under shallow-water conditions | Fig. 8A, B |
| **Muddy sandstone** | Sm | Muddy sandstone | Lenticular sets of cross-laminations, 1 to 30 mm thick, marked by mud drapes | c.0.3 m thick layers no more than 25 m in lateral extension | Abrupt transition at the base with lithofacies Sf and at the top with lithofacies M | Mutually erosive climbing type-A ripples deposited on the flood plain under shallow-water conditions | Fig. 8A, C |
| **Mudstone** | M | Bioturbated mudstone | Structureless | c.0.05 m thick layers no more than 2 m in lateral extension | Abrupt transition at the base with lithofacies Sm and erosive surface at the top with lithofacies Sl | Settling of mud on the flood plain under stagnant water conditions | Fig. 8A<br>Fig. 10C |
| **Palaeosol profiles** | P1<br>P2 | Parent material shows fining-upward trend from coarse-grained to medium-grained sandstone; colour varies gradually from reddish pink (10YR 7.0/2.5) at the top to light pink (10YR 8.0/1.5) at the bottom of the profile | Structureless. Bioturbation is observed in P1 and carbonate nodules in P2. | Tabular layers, more than 110 m in lateral extension and up to 1.25 m thick | Gradual vertical transition at the base with lithofacies S and erosive surface at the top | Incipient palaeopedogenesis associated with lithofacies Stc during relatively long periods of stability of the topographic surface characterised by absence of sedimentation | Fig. 4A, B<br>Fig. 10C, D, E |

**Table 1.** Description and interpretation of the lithofacies.

| Code | Architectural element | Sketch | Description | Lithofacies | Sequence | Figure |
|---|---|---|---|---|---|---|
| CF | Fining-up cross-bedded channel | 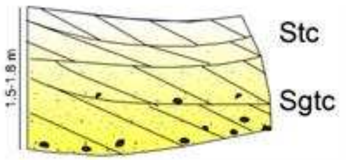  | Sheet sandstone beds showing fining-upward trend and upward increase in sorting. The element is composed of trough cross-bedded pebbly sandstone (Sgtc) at the base and trough cross-bedded sandstone (Stc) toward the top. Thickness varies from 1.5 to 1.8 m. It extends laterally for more than 100 m. The bottom and top bounding surfaces are erosional. | Sgtc - Stc | First sequence<br>Third sequence (only Stc) | Fig. 4C, D, E<br>Fig. 10A, B |
| CL | Lenticular cross-bedded channel | 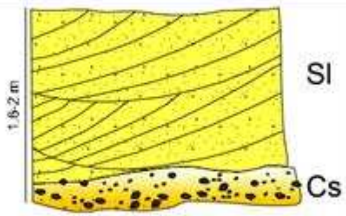  | Sheet sandstone beds formed by sandy conglomerate (Cs) at the base and large-scale lenticular cross-bedded sandstone (Sl) at the top. The lenticular cross-stratified sets do not show upward variation in dimension or grain size. Thickness varies from 1.6 to 2 m. It extends laterally for more than 100 m. The bottom and top bounding surfaces are erosional. | Cs - Sl | Second sequence | Fig. 9A, B, C |
| FL | Floodplain | 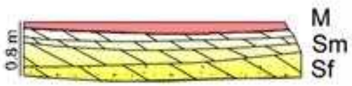  | This element consists of three lithofacies, organised in a fining-upward succession. From the base to the top: fine-grained sandstone (Sf), muddy sandstone (Sm) and mudstone (M). The element reaches 0.8 m vertically and is cut laterally by erosional surfaces of elements CF and CL. | Sf- Sm - M | First sequence<br>Second sequence (only M) | Fig. 8<br>Fig. 9C |
| P | Palaeosol | 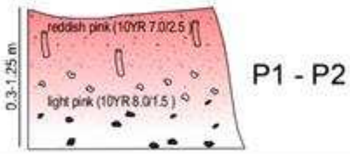  | This element if formed of palaeosol profiles (P1 and P2). The top bounding surface is erosional and the bottom limit is gradual to the element CF. It extends laterally for more than 100 m. Thickness varies from 0.3 to 1.25 m. | P1 - P2 | Below the first sequence (P1)<br>Top of third sequence (P2) | Fig. 4A, B<br>Fig. 10C, D, E |

**Table 2.** Description and interpretation of the architectural elements.

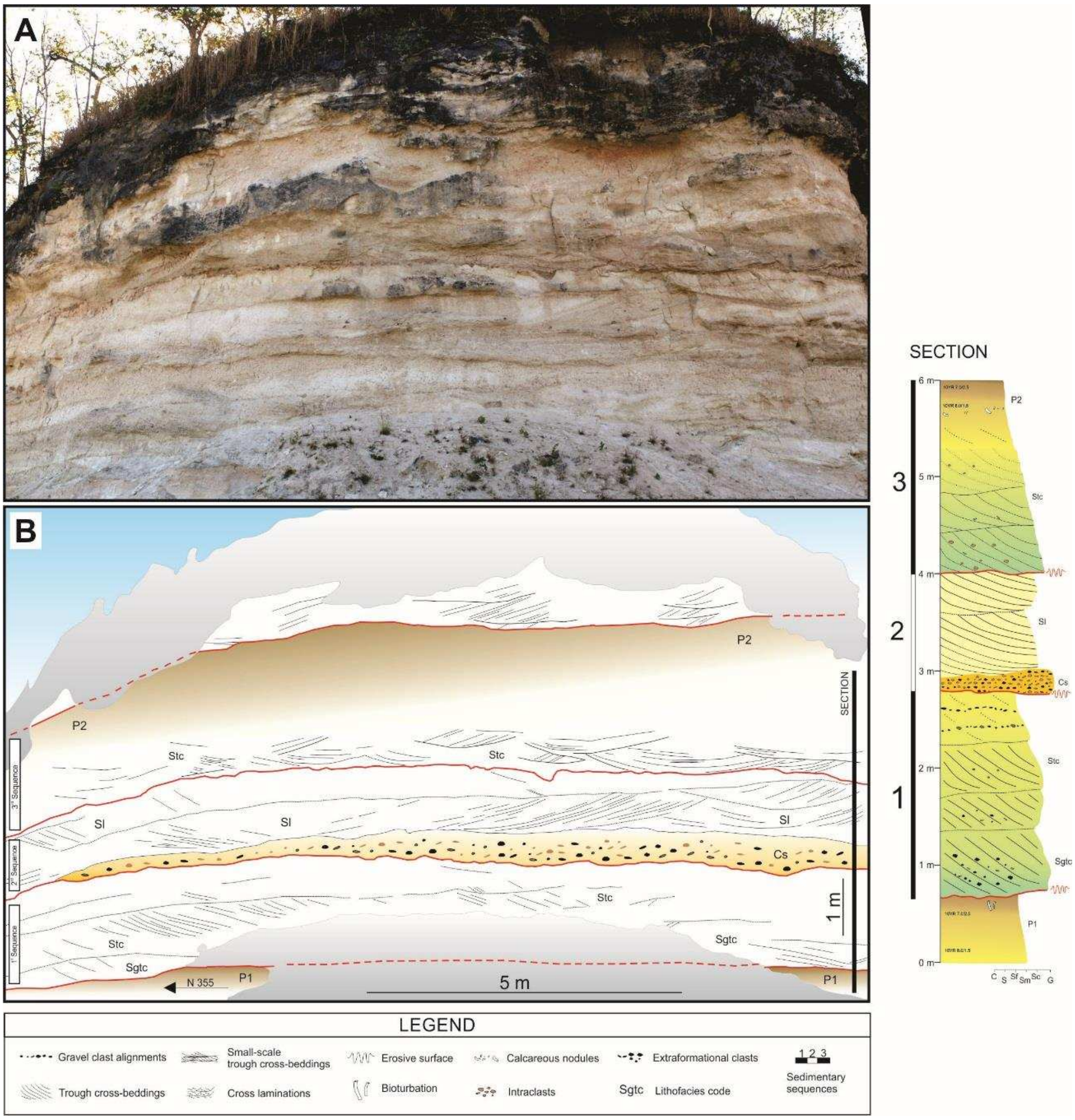


**Figure 5.** Architectural sketch and stratigraphic section of the studied sedimentary succession in view perpendicular to palaeoflow. The sketch shows the distribution of lithofacies in three channelised sequences. Channel deposits are bounded by palaeosols at the base (P1) and top (P2).

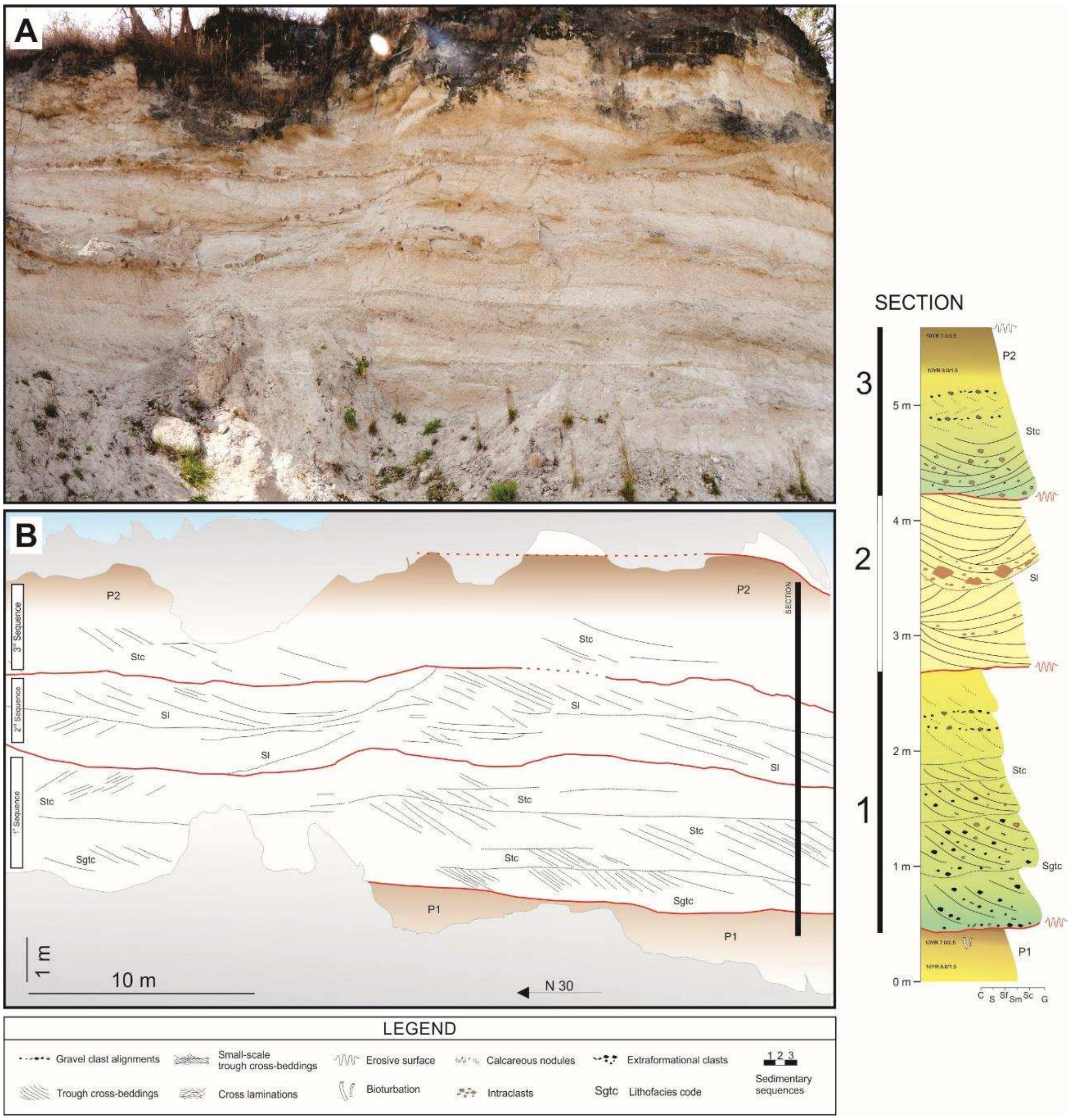


**Figure 6.** Architectural sketch and stratigraphic section of the studied sedimentary succession in palaeostreamwise view. The sketch shows the distribution of lithofacies in three channelised sequences. Channel deposits are bounded by palaeosols at the base (P1) and top (P2).

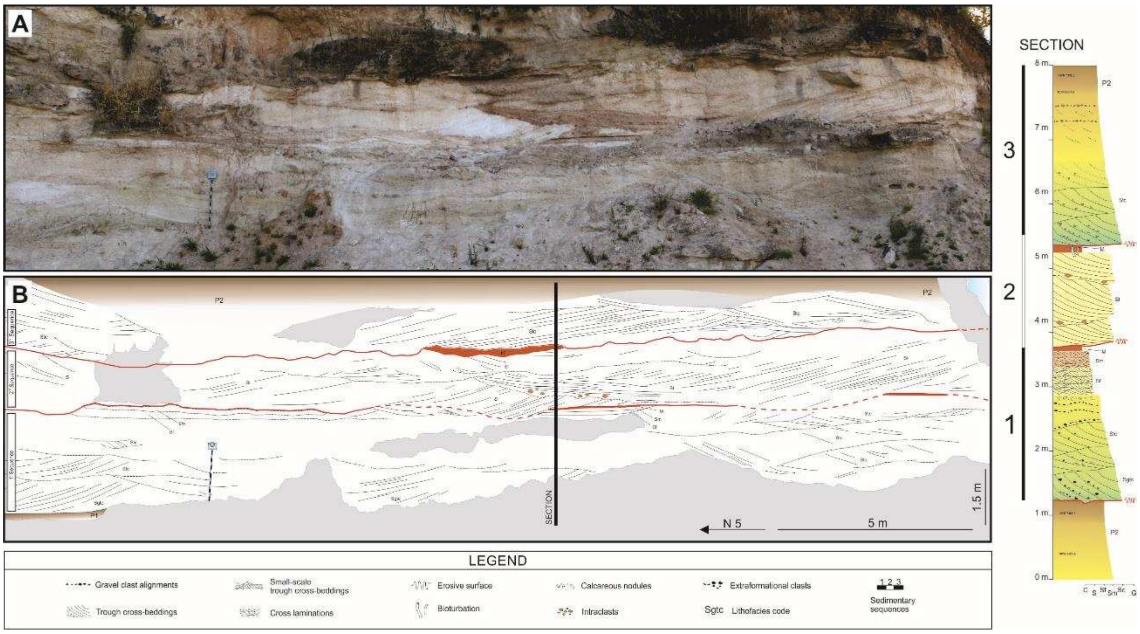


**Figure 7.** Architectural sketch and stratigraphic section of the studied sedimentary succession in palaeostreamwise view. The sketch shows the distribution of lithofacies in three channelised sequences. Channel deposits are bounded by palaeosols at the base (P1) and top (P2).

#### 4.1.2. Floodplain deposits

*Description.* Floodplain deposits occur at the top of this first sequence. These deposits constitute an architectural element (Floodplain Fl, Tab. 2) up to 0.8 m thick, partially or completely cut laterally by the erosional surface, which constitutes the bottom of the second sequence. This element is composed of three lithofacies, organised in a fining-upward succession. From the base to the top: fine-grained sandstone (lithofacies Sf), muddy sandstone (lithofacies Sm) and mudstone (lithofacies M) (Fig. 8A). The fine-grained sandstone is *c.* 0.5 m thick and made of sets that are 0.1 to 0.2 m thick, showing lateral pinch-out and composed of small trough cross-stratifications with foreset dip of 15-20°. Boundaries between sets are marked by accumulation of mudstone (Fig. 8B). Muddy sandstone overlays the previous lithofacies with a sharp transition. It forms a 0.3 m-thick interval of lenticular sets of cross-laminations, which are 1 to 30 mm thick. Boundaries between laminations are distinct due to the accumulation of mudstone (Fig. 8C). A structureless mudstone layer, 50 mm thick, constitutes the upper portion of this element (Fig. 8A). The bottom of this lithofacies is represented by a distinct and sharp surface. The mudstone shows bioturbation that consists of millimetre-thick tubes filled with muddy sandstone.

*Interpretation.* The fining-upward trend observed in these deposits evidences a constant reduction in flow energy. Taking in account the fine-grained nature of the sediments and the gradual transition from channelised deposits, this element can be interpreted as an overbank deposit (Miall, 2006). Initially, small three-dimensional sinuous dunes (lithofacies Sf) deposited on the floodplain under shallow-water conditions (Miall, 2006). The muddy laminae between sets and foresets indicate settling of muddy particles during episodes of stagnant water and/or oscillations of the flow. This suggests common and repeated interruptions of dune migration in response to falling water stages, caused by the return of floodwater back to the adjacent channel (Miall, 2006). The superimposition of mutually erosive climbing type-A ripples (lithofacies Sm) over the previous dunes records a channel shift away from its previous site (Jopling and Walker, 1968). The texture variations represent subaqueous flows dominated by low-energy alternations of episodic floods and stagnant water (Miall, 2006). The last stage of this sequence is recorded by mudstone (lithofacies M), indicating settling of mud under stagnant water conditions, further indicating the loss of channel influence as a response of the progressive shifting.

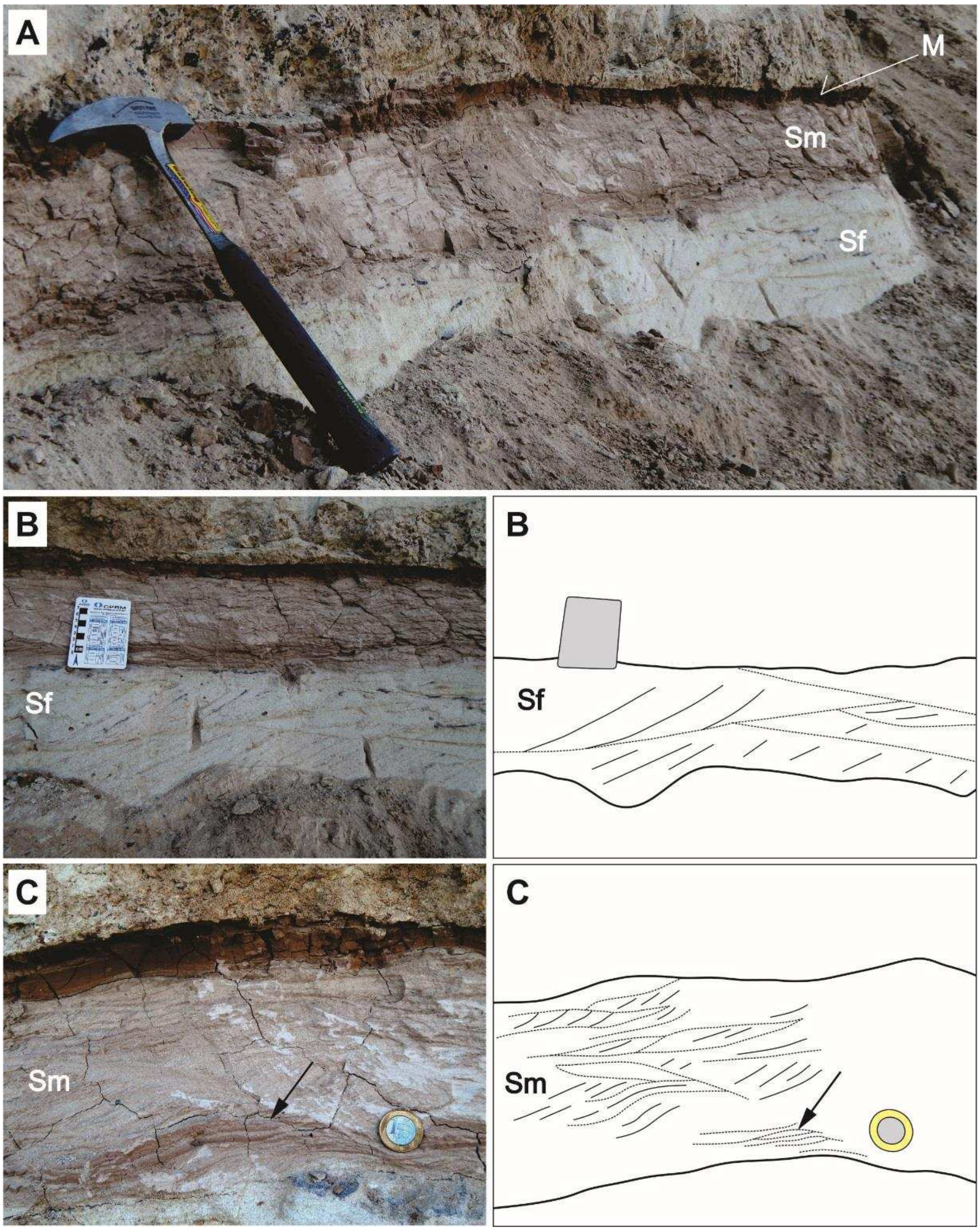


**Figure 8.** Floodplain architectural element (FL) of the first sequence. (A) This element is composed of a fining-upward small sequence, which is cosstituted, from the base to the top by fine sandstone (Sf), muddy sandstone (Sm) and mudstone (M). (B) Close-up of trough cross-bedded fine-grained sandstone (Sf). (C) Close-up of muddy sandstone showing interdigitated sets of light brown, cross laminations (Sm). The brown lines between sets and foresets underline mud drapes (see arrow).

## 4.2. SECOND SEQUENCE

The second sequence displays significant differences with the respect to the first sequence, with regards to both lithofacies characteristics and their vertical sequential order. This sequence is composed of a sheet-like sandstone body, which extends laterally for more than 100 m, is 1.6-2 m thick, is made of channel-fill deposits, and is covered by thin and isolated floodplain mudstone deposits. The bottom of the sequence is outlined by an undulose erosional surface, locally marked by large-scale (6 m wide and 0.5 m deep), symmetrical, concave-up scours (Fig. 7).

#### 4.2.1. Channel-fill deposits

*Description.* Channel-fill deposits take the form of a laterally extensive sheet-like unit, the lower erosive bounding surface of which overlies channel-fill and floodplain deposits of the first sequence. The architectural element that forms this channel fill (Lenticular cross-bedded channel CL, Tab. 2) is composed of two lithofacies: sandy conglomerate (Cs) and large-scale lenticular cross-bedded sandstone (Sl) (Fig. 5, 6 and 7). The lower portion of the channel-fill deposits consists of structureless, a matrix-supported sandy conglomerate tabular layer (lithofacies Cs, Tab. 1), more than 15 m in lateral extent, up to 0.5 m thick, and bounded by horizontal erosive surfaces at the bottom and the top (Fig. 9A, B). Conglomerate clasts include intraformational and extraformational elements. Extraformational clasts do not exceed 20 mm across; they are rounded to well-rounded, and are composed of quartzite, chalcedony and gneiss fragments. Intraformational clasts are composed of angular to sub-angular, pebble- to cobble-sized mudstone and small pebbles of pedogenic calcareous nodules. The sandy matrix is very coarse- to coarse-grained, with carbonate cement. The sandy conglomerate layer is characterised by progressive upward decrease of gravelly clasts, which possess a crude grading (Fig. 9B). Large-scale lenticular cross-bedded sandstone sets (lithofacies Sl, Tab. 1) overlie the sandy conglomerate and constitute most of the channel-fill deposits. The sandstone is poorly to moderately sorted, medium- to coarse-grained. Figure 2C presents the petrographic composition, which permits classification of the sandstone as a sublitharenite. Cross-strata have gentle dips (inclined 10-15°), are concave-up and wedge-shaped, and taper toward the toeset, which is tangential and long (Fig. 5, 6 and 7). In palaeostreamwise section, the sets are 10-15 m long and up to 1.4 m thick. The basal bounding surface is concave-up and the top is planar or mildly concave-up (Fig. 9C). Dip directions of the foresets indicate a palaeocurrent toward the northwest (Fig. 3). Reddish brown mudstone intraclasts are commonly concentrated at the base of the lenticular sets (Fig. 9D). In vertical section, two or three lenticular cross-bedding sets constitute the entire channel-fill sequence. No vertical variation of type or dimension of the sets is observed. Another noteworthy aspect of this second sequence is the absence of vertical organisation of this architectural element. The lenticular cross-bedded sets do not show upward variation in dimension or grain size, which contrasts with observations from the first sequence. In this second sequence, floodplain mudstone deposits abruptly overlie medium- and coarse-grained cross-bedded sandstone.

*Interpretation.* The erosive surface at the bottom of the second sequence suggests an environmental change from a low energy or calm water depositional environment on a floodplain to a renewed erosion and deposition within a channel system, probably provoked by avulsion (Allen, 1965). The lithofacies that comprise this architectural element indicate the restoration of subaqueous high-energetic environmental conditions, characterised by a channel with flow operating close to supercritical conditions. The sandy conglomerate (lithofacies Cs) indicates episodes of rapid deposition of bedload and suspended load reoccupying a previously active site of the channel belt. The erosive bottom, along with the crude normal grading, indicates transient turbulence associated with these flows. Turbulence causes coarser and denser clasts to settle from suspension directly onto the erosive bottom, creating a normally graded deposit (Nemec and Steel, 1984). The absence of stratification and abundant sandy matrix reveal rapid deposition of hyperconcentrated flow that inhibited any internal organisation (Costa, 1988).

The presence of large-scale lenticular cross-bedded sets indicates that channel-fill deposits from the second sequence were generated in hydraulic conditions different than the first sequence. Røe (1987) reported analogous lenticular cross-bedding sets from a Late Precambrian river system. These sets show thickness and streamwise length similar to those described here, and internally they are constituted of concave-up or sigmoidal, foresets dipping at 10-20 degrees. Røe (1987) interpreted these lenticular cross-bedding sets as dunes developed in response to high-velocity currents at the transition between the dune and upper-stage plane-bed fields. High flow conditions responsible for the generation of concave-up foreset are also described by Jopling (1965, see his Fig. 3), who observed experimentally that the increase of the flow strength yielded the modification of the lee-side profile of dunes from planar with angular bottomset through planar with tangential bottomset to low-angle concave-up. Jopling (1965) attributed the profile modifications to an increase of deposition from suspension on the lee side, which overcame the deposition for avalanching, itself confined on the upper part of the lee side. Indeed, the comparison with the lenticular cross-bedding of Røe (1987) does not fit perfectly to large-scale lenticular cross-bedded sets because the foresets described from this author display lateral variation of sigmoidal foresets, which were not observed into the second sequence. However, Chakraborty and Bose (1992), based on study of an ancient succession, reported a sequence of sedimentary structures formed by progressive increase of current strength from dune to upper-stage plane bed. In this model, cross-stratifications with low-angle and concave-up foresets deposited at the first phase of transition from dune to upper-stage plane bed.

In summary, the large-scale lenticular cross-bedded architectural element (CL) represents large dunes formed in higher fluvial current intensity and with larger amount of suspension material than the bedforms that comprise the first sequence. The permanent presence of large-scale lenticular cross-bedded sets without vertical variations of dimension and grain-size and their abrupt burial by mudstone suggests that the channel was characterised by the same hydraulic conditions until its sudden abandonment.

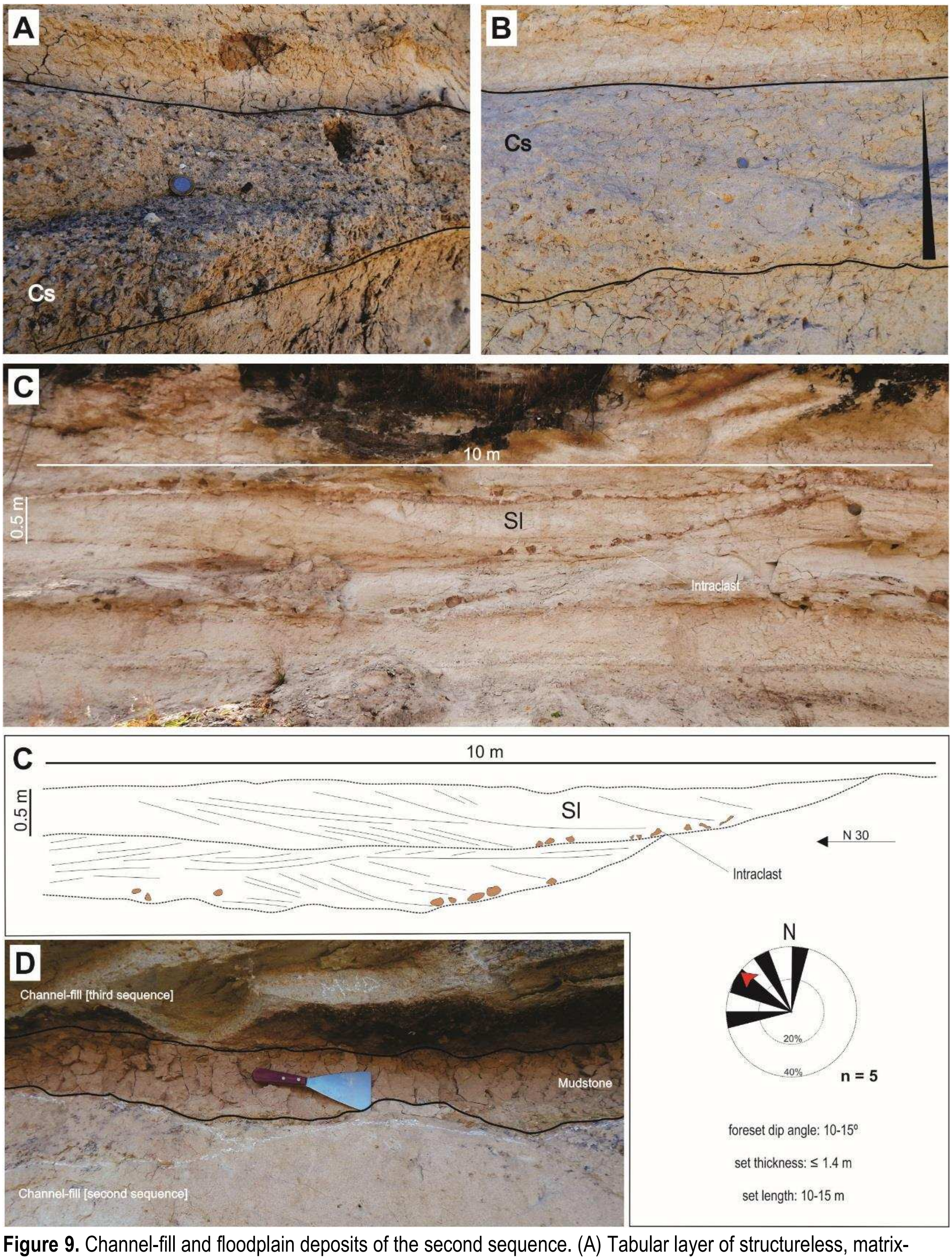


**Figure 9.** Channel-fill and floodplain deposits of the second sequence. (A) Tabular layer of structureless, matrix-supported sandy conglomerate which is constituted of extraformational and intraformational clasts. (B) Crude normal grading is locally observed in sandy conglomerate lithofacies (Cs). (C) Large-scale lenticular cross-bedded sandstone sets (Sl) showing low-angle, concave-up foresets. The bottom limit is outlined by concave-up scours with mudstone intraclasts. (D) Thin bed of structureless mudstone which overlays the channel-fill deposit of this second sequence.

#### 4.2.2. Floodplain deposits

*Description.* Floodplain deposits consist in thin, up to 0.4 m thick, no more than 3 m wide, beds of structureless mudstone (Fig. 9D). Local bioturbation, consisting of millimetre-scale tubes filled by fine-grained sandy silt, is present.
*Interpretation.* Mudstone corresponds to overbank deposition by suspended load in stagnant water conditions. This abrupt juxtaposition of mudstone on medium- to coarse-grained sandstone deposits suggests a sudden environmental change due to rapid abandonment of the channel. Furthermore, the intense bioturbation indicates a marked decrease of the environmental energy (Hubert and Hyde, 1982; Tunbridge, 1984; Miall, 2006).

## 4.3. THIRD SEQUENCE

The third sequence is formed by channel-fill deposits, which are 2.35 m thick, and whose upper portion is palaeopedogenised for 0.3 m. At the bottom, this sequence is delimited by an erosive surface; the top is delimited by another erosional surface that is superimposed by poorly exposed coarse-grained channelised deposits.

### 4.3.1. Channel-fill deposits

*Description.* The channel-fill deposits of the third sequence are represented by a sheet-like unit, more than 100 m in lateral extent. The layer is bounded at the bottom by an undulose erosional surface that overlies channel-fill and locally floodplain deposits of the second sequence. The surface shows small-scale asymmetrical erosive scours, which are 0.1 to 0.3 m deep and 0.5 to 1 m wide (Fig. 10A). The channel deposits are characterised by a fining-upward trend, from pebbly sandstone at the base to medium-grained sandstone at the top. The sorting of sandstone also increases upward, from poorly sorted to moderately sorted. This element (CF) can be divided in a lower and an upper portion. The lower portion is composed by pebbly sandstone beds with through cross stratifications, varying from 0.3 to 4 m wide and 0.2 to 0.6 m thick (Fig. 10A, B). Foreset dips record a unidirectional trend towards the northwest (Fig. 3). The bounding surfaces of the sets and foresets are marked by the accumulation of granules and pebbles of mudstone intraclasts (Fig. 10A). The uppermost portion consists of medium-grained, apparently structureless sandstone in which there occurs the horizontal alignment of granules and cobbles of mudstone intraclasts. These larger clasts are arranged parallel to the bounding surfaces of sets (Fig. 10B). The transition between the lower and upper portion is gradual.
The top of the channel-fill deposit is overlain by a 0.3 m-thick palaeosol (lithofacies P2), which comprises moderately sorted, fine-grained sand (Fig. 10C). The palaeosol profile (architectural element P) shows vertical colour variation from reddish pink (10YR 7.0/2.5) at the top to light pink (10YR 8.0/1.5) at the bottom (Fig. 10C) and is attributed to rust coatings on quartz grains. Subspherical carbonate nodules, 1 to 150 mm across, are less than 10% in abundance and concentrated on a horizon approximately 0.4 m below the top of the profile (Fig. 10D). Nodules are composed of micritic calcite with floating medium-grained sand clasts. Mottles are commonly dispersed near the top; they are irregular in shape and white in colour (7.5YR 8/1) (Fig. 10E).
*Interpretation.* The erosive surface that divides this sequence from the floodplain deposits of the second sequence indicates reactivation of a channel over a previously abandoned channel system (Miall, 2006). The channel-fill deposits share similar characteristics encountered in the first sequence. Correspondingly, the sandstone (lithofacies Stc; architectural element CF) results from the migration and deposition of three-dimensional dunes with sinuous crests. The palaeohydrological behaviour is similarly controlled by steady and waning flow. The accumulation of intraformational mudstone granules to cobbles along horizontal surfaces corresponds to lags, resulting from the winnowing of finer sediments during episodes of higher water discharge and low sediment deposition (Miall, 2006). The higher concentration of intraclasts indicates cannibalistic behaviour of the fluvial system on

floodplain deposits at this stage of deposition. The absence of sedimentary structures in the uppermost part of the sandstone is in part related to the increase in sorting and in part to palaeopedogenesis, as suggested by carbonate nodules, mottles and bioturbation observed in the upper portion of the sequence.
The palaeosol profile at the top of the third sequence marks a relatively long period of inactivity of the channel system in this area (Retallack, 1988). The vertical colour intensification toward the top of the profile indicates rubification (Fenwick, 1985), as similarly observed in the palaeosol below the first sequence. The absence of horizons and the reduced thickness of the profile suggest a relatively short time (no more than $10^3$ y) of development of the palaeosol.

## 5. FLUVIAL PALAEOHYDROLOGY AND DEPOSITIONAL HISTORY

The studied succession exhibits three superimposed sequences of fluvial deposits characterised by different depositional features, suggesting variations in the palaeohydraulic conditions. Peculiar aspects are shown by lithofacies and architectural organisation of the beds: (i) the deposits are composed of immature, poorly sorted, coarse-grained clastic sediments organised in sedimentary lithofacies mostly related to unidirectional high-energy flows (Tab. 1), (ii) floodplain deposits are scarce (Fig. 3), as a result channel deposits are commonly amalgamated, (iii) the bottom and the top of the three sequences are marked by palaeosol profiles (Fig. 5 and 6). Sedimentological features of these deposits and their stratigraphic organisation suggest that these deposits are part of the more proximal portion of a fluvial distributive system.
The sequential analysis of the interval displays important palaeohydraulic variations of the channels through time. Each sequence relates to episodes of channelisation characterised by waning flows of varied conditions in hydraulic power, stability, sediment saturation and erosive potential. The sharp superposition of floodplain deposits over channel fills and the absence of any indicators of lateral migration suggest that transitions between episodes of channel cut-and-fill occurred through sudden avulsions of the channels. The palaeosol profiles, which bound the study succession at the base and the top, indicate relatively long cessations in fluvial sedimentation during episodes of stable surface conditions (Fig. 3).

### 5.1 First sequence

The deposition of the first sequence commenced with the incision of a river channel over a stable floodplain surface. This is evidenced by the erosion of a palaeosol profile, which suggests previous stable conditions of the topography for at least for several hundred years and more likely thousands (Fig. 11A). In-channel deposition began with a wide dune field (lithofacies Sgtc; architectural element CF), characterised by superimposed migrating bedforms with sinuous crests (Fig. 11B). Subsequently, flow energy and depth decreased progressively, forming smaller three-dimensional dunes (lithofacies Stc; architectural element CF), until the channel was completely filled. The lithofacies assemblage indicates that the channel was characterised by steady and subcritical flow conditions with permanent water flow. Previous researches (Basilici et al., 2009; Dal Bó et al., 2010; Basilici and Dal Bó, 2010a), using palaeosol proxies, defined the climate of the Upper Cretaceous of the Bauru Basin as semiarid, but characterised by low-period oscillations between more humid and drier phases. In this context, the steadier behaviour of the flow inferred for the first channel deposit can be linked to a more humid episode, characterised by seasonal rainfall and higher groundwater level (Tooth, 2000). In systems subject to seasonal climates, dryland rivers are subject to periodic floods, which elevate the groundwater level, maintaining channels with a steadier behaviour in water discharge (Graf, 1988; Cooke et al., 1993; Meredith et al., 2015). Progressive sediment filling (ckoking) encouraged the final abandonment of the channel. The channel is filled by sediments that are characterised vertically upward by a gradual decrease in grain size and thickness of crossstratificatified sets. This demonstrates a progressive temporal decrease in the dimension of the dunes present in the channel, indicative of a progressive temporal decrease of the flow intensity. In the upper part of the sequence, the floodplain deposit records gradual abandonment of the channel. When the channel was still close-by, overbank flows deposited small three-dimensional dunes, later covered by mud laminae settled during falling water stages between floods. Several floods and falling water stages are recorded within the overbank deposits, indicating the oscillatory hydraulic character of the fluvial system, controlled mainly by flood events. Due to a progressive shift of the active channel, a second depositional stage is indicated by the alternating deposition of ripples and mud laminae on top of the deposits of the older dune field. The last stage of overbank deposition occurred in a distal floodplain environment: fine particles settled from standing water in temporary ponds (Meredith et al., 2015). The fining- and thinning-upward trend of floodplain deposits provides indirect evidence of avulsion. The avulsion process occurred in stages along a more gradual migration where the main channel diverted from its original locus to a distal area of the floodplain.

### 5.2. Second sequence

The sedimentation of the second sequence developed over an erosional surface again suggesting an abrupt environmental shift due to channel avulsion (Kraus and Wells, 1999). The lack of palaeosol profiles between the first and the second sequences indicates short recurrence time between channel abandonment and reoccupation, possibly indicating a high-frequency avulsion behaviour of the fluvial system. Fluvial deposition within a second channel commenced with episodes of rapid deposition by hyperconcentrated flows (lithofacies Cs; architectural element CL) over the previously abandoned channel. The well-developed roundness of pebble-sized clasts probably indicates cannibalism of older fluvial deposits during channel reoccupation (Nemec and Steel, 1984). After the first stage, subsequent filling was established by the migration of large dunes (lithofacies Sl; architectural element CL) during intense and fast-changing floods operating under a transitional regime close to upper-flow stage (Fig. 11C) (Røe, 1987; Chakraborty and Bose, 1992; Fielding, 2006). Conditions transitional to upper-stage plane-bed bedforms can develop where the flow velocity is high enough. However, the presence of large dune deposits in the geological record is due to particular hydraulic conditions where a rapid decline of the flow regime does not permit a re-equilibrium of the bedforms to structures of lower regime (Jones, 1977). Thus, sedimentary structures of upper flow regime and transitional to upper flow regime are preserved in fluvial systems characterised by a sharp variation of the hydraulic regime (Plink-Björklund, 2015). This does not necessarily mean that these rivers had an "ephemeral" character, but that they were subject to marked variations of hydraulic regime, as for example in climate conditions characterised by strong seasonal rainfall (Fielding, 2006). Within the deposits of this channel, wind-ripple laminations, current or wave ripples, signs of initial pedogenesis, mud drapes, thin sandstone beds and planar laminations were not identified. These depositional features would record evidence for emergence or stagnant shallow water and constitute attributes typical of ephemeral rivers (Reid and Frostick, 2011). Thereby, the absence of this evidence seems to exclude the ephemeral character for this channel system and more likely suggests a river with strong variation of hydraulic regime. the high abundance of mudstone intraclasts demonstrates an increase in the cannibalistic behaviour of the river over its floodplain area during flood episodes.

The superposition of mudstone over the coarse-grained channel deposits provides indirect evidence of sudden abandonment of the active channel by avulsion (Slingerland and Smith, 2004). After channel avulsion, sedimentation took place by settling of mudstone under standing water conditions in distal floodplain area. When compared to the first channel, this avulsion episode might record a more rapid channel abandonment likely in response to a rapid shift of the active channel from its former site.

## 5.3. Third sequence

Another sudden river avulsion marked the transition to the third sequence. The absence of palaeosol profiles at the top of the second sequence records a short recurrence time of the river avulsion. The third channel deposit exhibits a depositional history analogous to the first: this channel deposit relates to a steady flow marked by deposition of a field of three-dimensional dunes with steady decrease in water discharge, which reflects gradual decline in flow depth and energy (Fig. 11D). As for the first channel deposit, this third channel deposit seems to be associated with a more humid episode for which seasonal rainfall and the elevated groundwater level contributed to permanent and steady discharge regime (Tooth, 2000; Meredith et al., 2015). Floodplain deposits on top of the sequence are not preserved because of palaeopedogenesis (lithofacies S). This suggests that the channel shifted position by a larger distance on the floodplain, leaving the region in the vicinity of the study area without direct fluvial depositional influence for a relatively long time. Coarse-grained channelised deposits (not described in detail here) overlie this palaeosol profile, indicating subsequent channel reoccupation of the area (Fig. 10B).

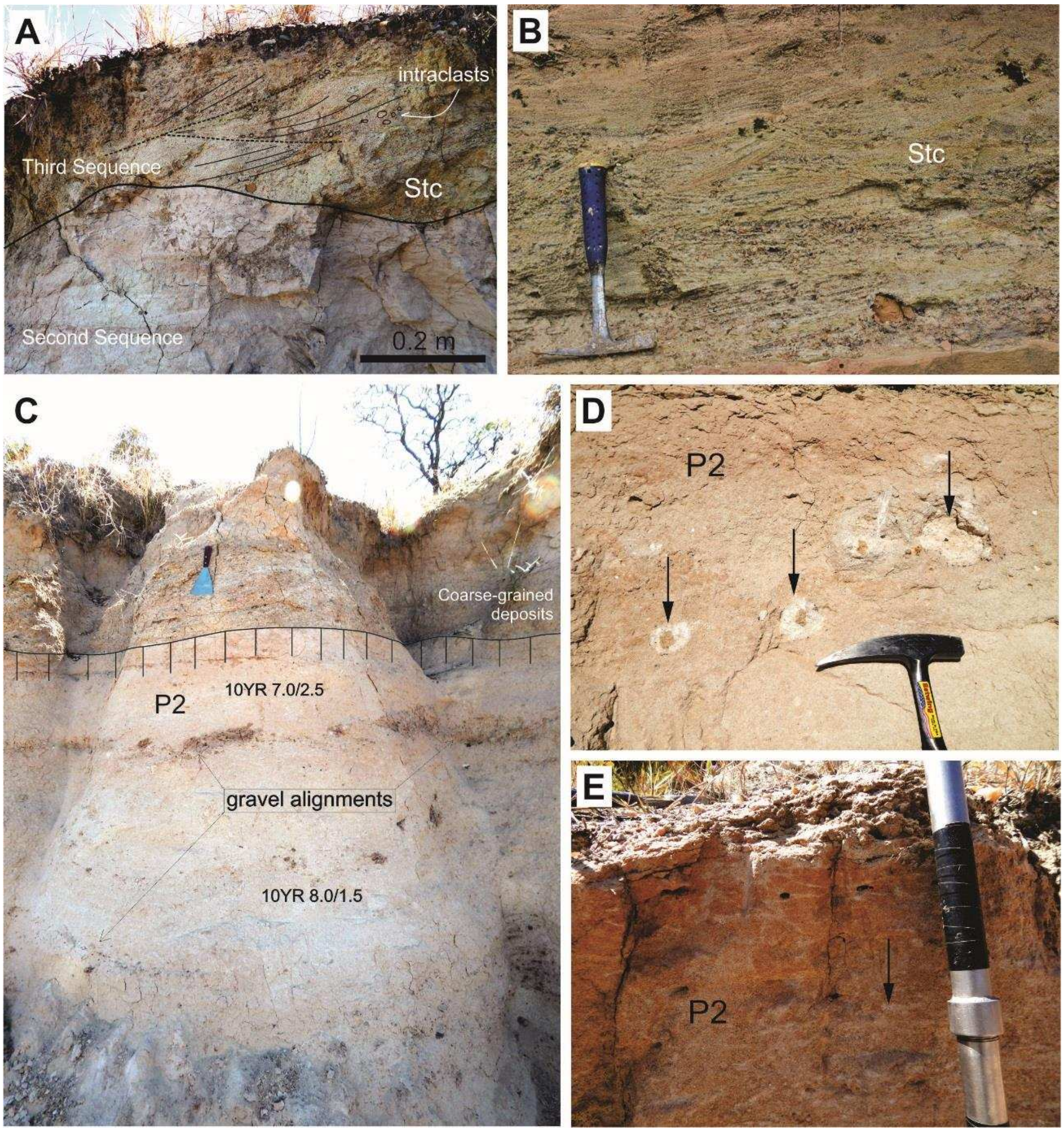


**Figure 10.** Third sequence. (A, B) Lowermost part of the sequence showing an erosive bottom, which is overlaid by trough cross-bedded conglomeratic sandstone (Stc) showing a high concentration of mudstone intraclasts.

(C) Palaeosol profile (P2) at the top of the third sequence showing vertical colour variation from reddish pink (10YR 7.0/2.5) at the top to light pink (10YR 8.0/1.5) at the bottom. Coarse-grained channelised deposits overlie the third sequence. (D) Subspherical calcareous nodules composed of pedogenic micritic calcite. (E) White-coloured irregular mottles near the top of the palaeosol profile (P2).

## 6. CLIMATE-INDUCED CYCLES ON FLUVIAL PALAEOHYDROLOGY

The tabular shape of the channel bodies remains unaltered throughout the study succession. This might suggest a constant tectonic condition (Allen et al., 2014). By contrast, substantial variation of the internal architecture and facies composition and arrangement of the fill of the channel elements is observed. This can be attributed to climate variations. The facies analysis of the three fluvial sequences has allowed reconstruction of the palaeohydraulics of the system and the depositional history of three superimposed channels. Small-scale sinuous-crested dunes, which are organised in fining- and thinning-upward sequences in the first and third channel fills (Fig. 11), record dune fields and suggest more stable and perennial river flow discharge. By contrast, large-scale, low-angle lee side, flattened dunes of the second channel fill, which were generated close to supercritical conditions, indicate higher velocity of the flow and irregular discharge. Thus, the three sequences of channel deposits suggest temporal oscillations of the river flow regime.

Similar palaeohydraulic variability has been described on modern rivers from Australia (Tooth, 1999), Israel (Schick, 1993) and South Africa (Tooth and Nanson, 1995), and mark a common behaviour associated with dryland (arid to dry-subhumid regions) fluvial environments (Tooth, 2000). The main cause that acts on the steadiness of river flow relates to the spatio-temporal distribution of rainfall (Graf, 1988). In more humid periods, drylands are characterised by multiple peaks of high rainfall that force the rivers to experience repeated floods. As consequence of persistent overbank infiltration after each flood, groundwater table rises up and establishes a hydraulic connection to rivers that are now recharged by the dryland aquifer system (Meredith et al., 2015). The influx from the groundwater to the channels provides the steadier flow conditions observed during more humid periods. Alternatively, drier periods are marked by scarce episodes of intense and isolated rainfall, whose contribution is insufficient to induce groundwater-table rise; therefore, no hydraulic connection is established between the channels and the dryland aquifer (Meredith et al., 2015). In drier climate conditions, the land surface shows an uneven vegetation cover and rainfall has high erosional effectiveness (Thornes, 1994). Overland flows, which act as main sources for rivers recharge, provide much of the sediment and, in particular, such flows liberate mudstone intraclasts and pedorelicts, which are mobilised from the floodplain deposits. A high abundance of mudstone intraclasts signifies the cannibalistic behaviour of the second channel fill. This feature – like the presence of structures interpretable as having been deposited at the transition to upper flow regime dunes, abundant mud clasts and absence of fining-upward filling – suggest that the deposition on the second channel fill took place when a drier climate period controlled the fluvial environment. Consequently, the studied fluvial succession is interpreted to have formed under the influence of a climate regime that alternated cyclically from relatively more humid to more arid.

Climate oscillations from more humid to drier conditions have been inferred by interbeddings of palaeosols and deposits in stratigraphically related successions of the south-eastern and north-western parts of the Bauru Basin (Fig. 12). In the north-western part of the basin, a detailed study on cyclic interbedding of aeolian sediments and palaeosols attributed these alternations to short-time scale fluctuations between a drier and a more humid climate (Basilici et al., 2009; Dal' Bó et al., 2010; Basilici and Dal' Bó, 2010). Drier episodes were characterised by aeolian sand sheet deposition, whereas more humid periods resulted in topographic stability with growth of vegetation and pedogenesis. Palaeoprecipitation estimates, using the CIA-K proxy (Nesbitt and Young, 1982), indicated *c.* 900 mm/y for more humid episodes and *c.* 240 mm/y for the drier episodes (Dal' Bó et al., 2010). In the south-eastern part of the Bauru Basin more humid episodes were associated with unconfined flood activity on the distal plain of a distributive fluvial system, whereas dry periods were related to an absence of fluvial sedimentation and development of pedogenesis (Basilici et al., 2016a). In this area, mean annual precipitation rates inferred from the depth of nodular Bk horizon in palaeosols range from 200 to 300 mm (Dal' Bó et al., 2009), indicating arid to semiarid conditions characterised by isolated and scarce episodes of rainfall.

During the relatively more humid episodes of the Upper Cretaceous of the Bauru Basin, ephemeral fluvial deposits were described in the north-western part of the basin (Basilici et al., 2009) and sheet-like flood deposits are recorded in the south-eastern part (Basilici et al, 2016a).

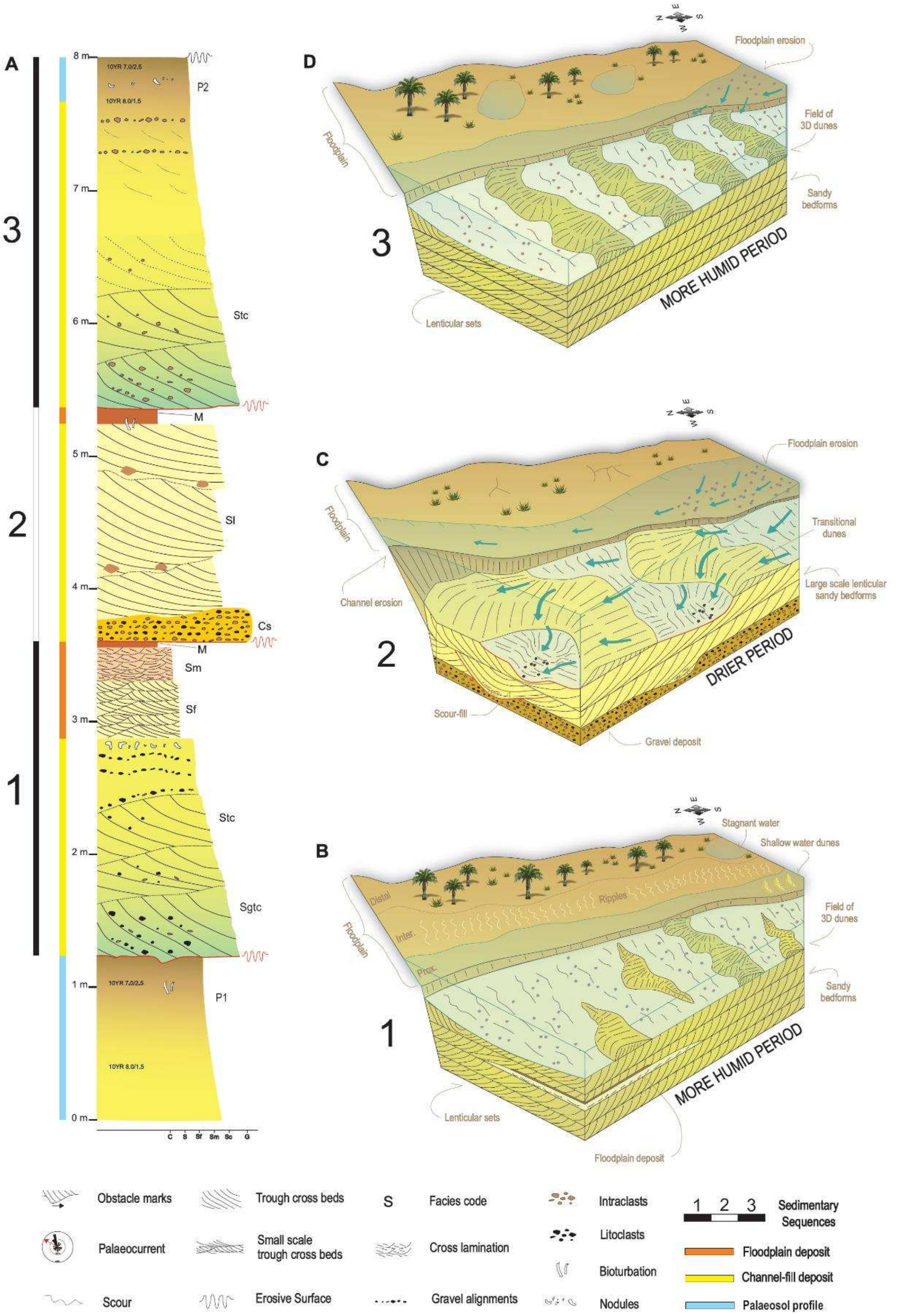


**Figure 11.** (A) Stratigraphic section showing three fluvial sedimentary sequences bounded by palaeosols at the base and the top. (B) This model reconstructs the first channel system, which was active during the more humid periods. The picture shows three-dimensional dunes with sinuous crests (Stc). Floodplain environment is associated with small three-dimensional dunes (Sf - proximal floodplain), ripples (Sm - intermediate floodplain) and stagnant water bodies (M - distal floodplain). (C) Reconstruction of the second channel system, active during drier periods, characterised by high-energy and erosive floods, which formed large and flattened dunes near supercritical conditions (Sl). (D) Reconstruction of the third channel system, which represents the return of a more humid climate period similar to the first sequence.

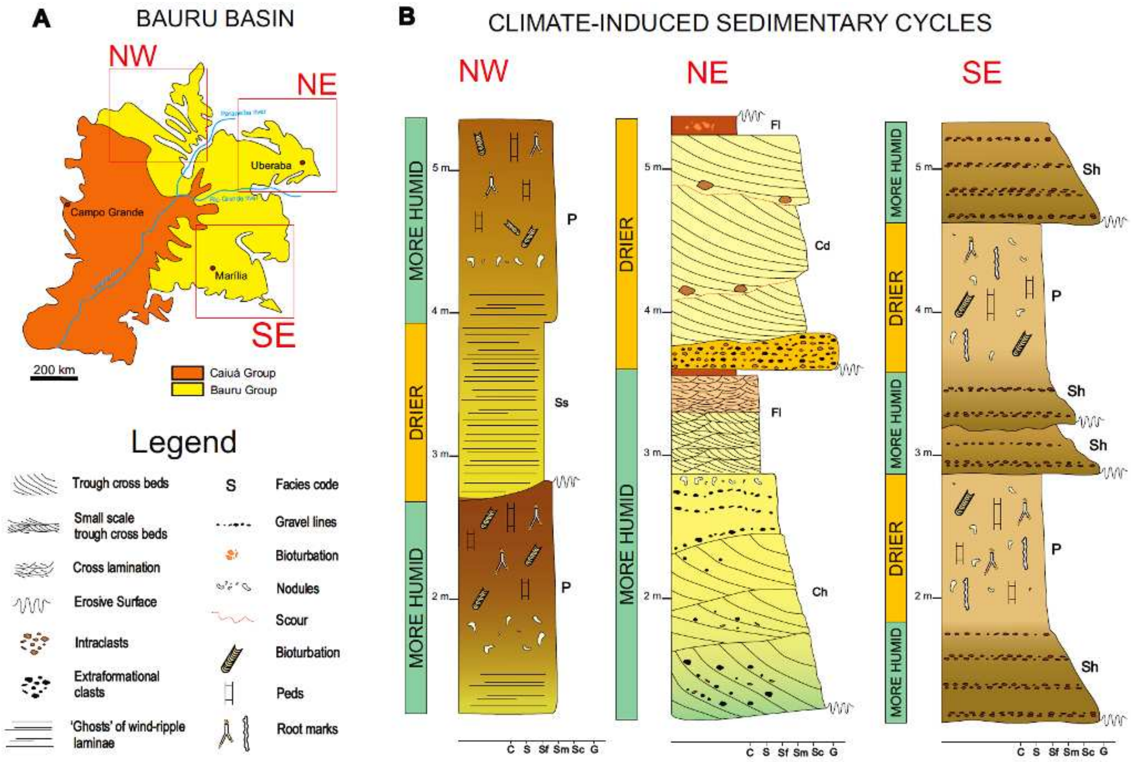


**Figure 12.** Climate-induced sedimentary cycles observed in northwestern (NW), northeastern (NE) and southeastern (SE) portions of the Bauru Group. The northwest portion (NW) shows alternation between palaeosols (P) and aeolian sand sheet (Ss) alternatively deposited during more humid and drier periods, respectively (see Basilici et al., 2009). Deposits in the northeast area (NE - this study) expose channel deposits that testify to steadier river flow during the more humid periods (Ch) and channel deposits yielded by ephemeral and energetic flows during the drier periods (Cd). The southeast portion (SE) of the basin reveals alternation between palaeosols (P) formed in drier period interbedded with sheet flood deposits (Sh) developed during more humid conditions (see Basilici et al., 2016a).

## 7. GEOMORPHOLOGIC CYCLE ON FLUVIAL DYNAMICS

Three amalgamated sandy sheet-like channel deposits composed the fluvial record. The distinct internal architecture of channel bodies is interpreted as the result of hydraulic variations in fluvial discharge. Furthermore, we interpret climate as the main factor controlling these changes of in-channel hydraulics. The bottom and the top of this succession of channels are delimited by palaeosol profiles, which indicate relatively long periods of stability of the topographic surface and absence of sedimentation (Kraus, 1999). The two palaeosol profiles identify an external architectural organisation of the study succession, suggesting a long-term shift of the channel-belt to relatively distant positions on the alluvial surface. The inferred sudden diversion of a channel-belt to a new position on the alluvial surface (avulsion *sensu* Allen, 1965) is a pivotal mechanism on the construction of the alluvial architecture. Avulsion processes have been widely described in the geological record and are interpreted as the sudden or gradual relocation of rivers to more topographically depressed positions on the floodplain (e.g., Allen, 1965, 1968; Bridge and Leeder, 1979; Leeder, 1978). Trigger mechanisms of avulsion include autogenic and allogenic processes. Autogenic (intrabasinal) processes include rapid channel aggradation, substrate composition and decrease in channel capacity (Makaske, 2001; Aslan et al., 2005), whereas allogenic (extrabasinal) triggers are associated with tectonics, eustasy and climate change mechanisms (e.g., Beerbower, 1964; Holbrook et al., 2003). The studied fluvial succession records a succession of three amalgamated sandy channel fill elements, indicating systematic reoccupation of the same area for the channel belt. This pattern of stacked sandy channel bodies has been identified in other ancient and modern fluvial deposits, and is associated with erodible sandy substrates as the controlling factor in avulsion (Maizels 1990; Kraus 1996; Kraus and Gwinn 1997; Makaske et al. 2002). Because channels aggrade, channel-belts become elevated and gravitationally unstable ridges (Tornqvist and Bridge, 2002). This geomorphologic condition forces the fluvial system to avulse to a new position on a laterally lower portion of the floodplain (Fig. 13) (Jones and Schumm, 1999; Slingerland and Smith, 2004). The occurrence of the three stacked channel bodies (Fig. 13B, C) could be explained by the development of an alluvial ridge and the consequent operation of morphologic and autogenic mechanisms that forced the channel-belt to avulse. The palaeosols (Fig. 13B, D), localised at the bottom and top of the succession of the three channels, indicate relatively long inter-avulsion periods (*sensu* Stouthamer and Berendsen, 2007). Influence of tectonic factors as possible drivers to river avulsion is not supported by the basin history of the upper part of the Bauru Group, which was characterised by low rates of generation of accommodation space (Basilici et al., 2016a). As a result, the studied succession is interpreted as most likely recording the superimposition of two different types of sedimentary cycles: (i) a high-frequency cycle controlled by allogenic climate factors which yielded different types of fluvial deposits (Fig. 13E), and (ii) a low-frequency cycle controlled by autogenic morphological factors, which allowed the development of an alluvial ridge.

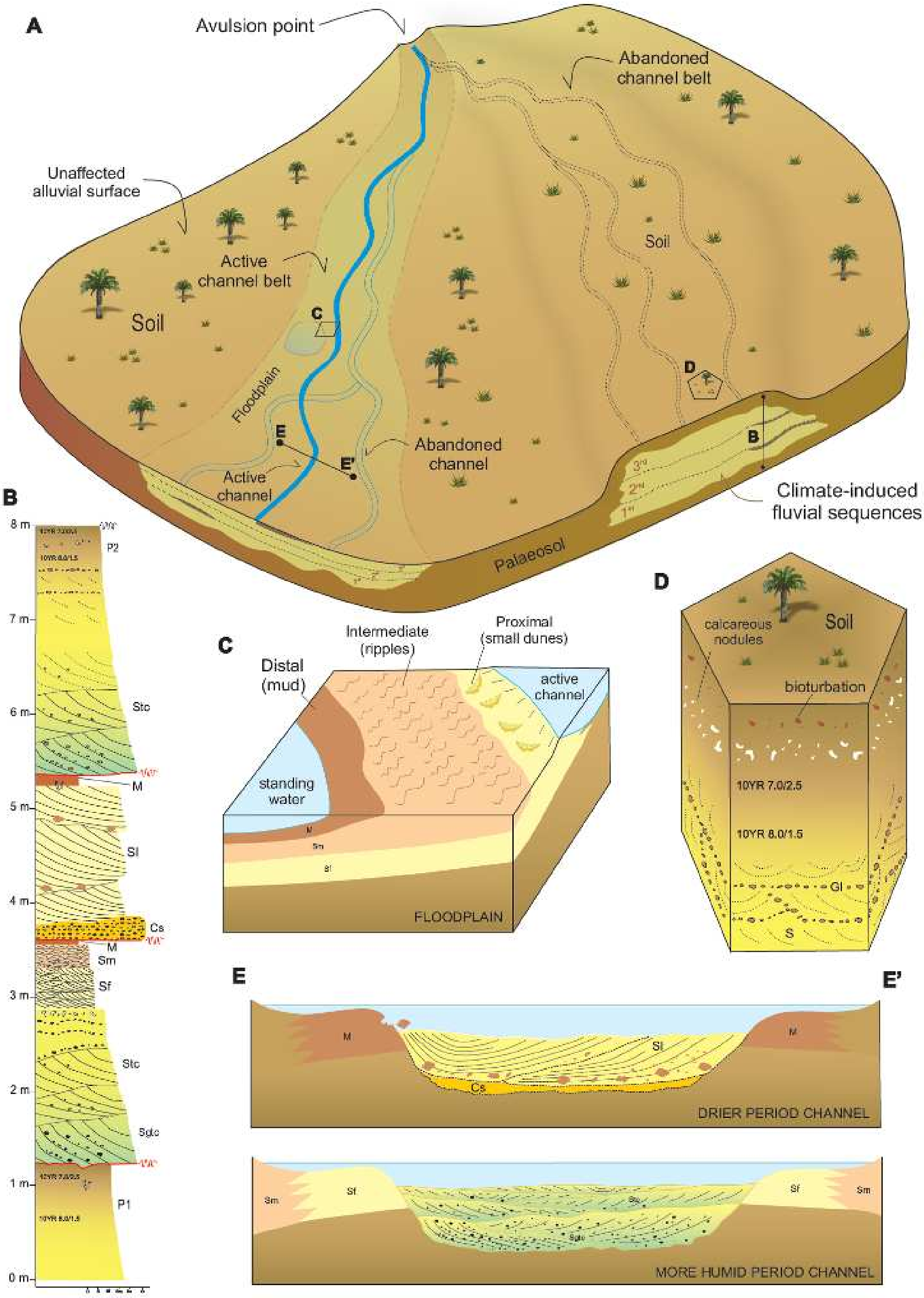


**Figure 13.** (A) Depositional model illustrating how geomorphology superimposes the climate-induced fluvial cycles and controls the lateral and vertical organisation of the studied fluvial succession. The channel belt containing laterally shifting channel is abandoned to a new distally lower position on the alluvial surface. (B) Detail to the stratigraphic product of climate-driven fluvial cycle superimposed by the longer-term geomorphologic fluvial cycle where fluvial sequences are bounded at the base and the top by palaeosols. (C) Detailed block diagram of the proximal, intermediate and distal parts of the floodplain. (D) Palaeopedon reconstruction showing main palaeopedogenic features of palaeosols (P1) and (P2). (E) Idealised cross-sections of channel deposits during more humid and drier periods. The channel fill associated with the drier period is developed as a lenticular cross-bedded channel architectural element (CL). periodThe channel fill developed during a more humid interval is developed as a fining-up cross-bedded channel architectural element (CF).

## 8. CONCLUSIONS

The upper portion of the Bauru Group near Peirópolis records the sedimentation of the proximal portion of a dryland distributive fluvial system wherein climate and geomorphology influenced its internal and external architecture, respectively. Three vertical fining- and thinning-upward sedimentary sequences have been recognised, each one constituted of channel and floodplain deposits. This alluvial succession is bounded at the bottom and the top by thin and few developed palaeosol profiles, whereas each sequence is separated by an erosive surface. Channel deposits are characterised by two types of internal architecture that suggest different hydraulic regime: (i) the first and the third channel deposits were formed by three-dimensional dune field deposits, which suggest floods with perennial and steady flow followed by falling flow conditions; (ii) the second channel fill was characterised by larger and flattened dunes with low-angle foresets, which testify to energetic and fast-changing floods operating close to supercritical conditions. The first type has been associated with more humid climate conditions, brought about by abundant and steady rainfall with probable groundwater contribution to the fluvial regime. The second type has been interpreted as related to drier periods with intense and transient episodes of exceptional rainfall. Therefore, it is possible to recognise a high-frequency climate control trough the internal architecture of the fluvial deposits. Similar high-frequency more humid-drier climate oscillations have been identified in Bauru Basin in adjacent portions of the study area, wherein they controlled alternating processes of pedogenesis and sedimentation of varied depositional systems. The succession of the three channel deposits is outlined at the bottom and top by two palaeosol profiles. These palaeosols testify to an interruption of the depositional processes and to the dominance of pedogenesis on the floodplain, due to shifts of the channel-belt to a distant position. The studied succession, delimited by the two palaeosol profiles, indicates a superimposed longer-term geomorphologic-depositional cycle probably controlled by the autogenic lateral dynamics of the fluvial system. Thereby, the studied succession is characterised by allogenic high-frequency climate-induced cycles that are superimposed to autogenic low-frequency geomorphologic-induced cycles. This study demonstrates that the internal architecture of channel deposits can be used to disclose palaeoenvironmental climate conditions and variations where other geological features are not available as climate proxies. In particular, internal channel architecture constitutes a compelling climate proxy in succession with high sedimentation rate (as in a fluvial belt) where low-developed palaeosol profiles do not permit a clear definition of the palaeoclimate conditions.

## ACKNOWLEDGEMENTS

The Editor, Brian Jones, and two anonymous referees are thanked for the constructive recommendations that have significantly improved the original manuscript. We would like to thank FAPESP (fellowship 2016/06968-5), CNPq (fellowship 132001/2016-0) for providing financial support to the first author, as also FAPESP (project n. 2012/23209-0) and CNPq (project n. 474227/2013-8) for sustaining the scientific activity of the second author.

## REFERENCES

Abdullatif, O.M., 1989. Channel-fill and sheet-flood facies sequences in the ephemeral River Gash, Kassala, Sudan. Sedimentary Geology, 63, 171-184.

Allen, J.R.L., 1965. A review of the origin and characteristics of recent alluvial sediments: Sedimentology, 5, 89-191.

Allen, J.R.L., 1968. The nature and origin of bed-form hierarchies. Sedimentology, 10, 161-182.

Allen, J.P., Fielding, C.R., Gibling, M.R., Rygel, M.C., 2014. Recognizing products of paleoclimate fluctuation in the fluvial stratigraphic record: an example from the Pennsylvanian to lower Permian of Cape Breton Island, Nova Scotia. Sedimentology, 61, 1332-1381.

Almasrahy, M.A., Mountney, N.P., 2015. A classification scheme for fluvial–aeolian system interaction in desert-margin settings. Aeolian Research, 17, 67-88.

Aslan, A., Autin, W.J., Blum, M.D., 2005. Causes of river avulsion: insights from the Late Holocene avulsion history of the Mississippi River, U.S.A. Journal of Sedimentary Research, 75, 648-662.

Bacchi, V., Recking, A., Eckert, N., Frey, P., Piton, G., Naaim, M., 2014. The effects of kinetic sorting on sediment mobility on steep slopes. Earth Surface Processes and Landforms, 39, 1075-1086.

Basilici, G., Dal' Bó, P.F.F., Ladeira, F.S.B., 2009. Climate-induced sediment-palaeosol cycles in a Late Cretaceous dry aeolian sand sheet: Marília Formation (north-west Bauru Basin, Brazil). Sedimentology, 56, 1876-1904.

Basilici, G., Dal' Bó, P.F.F., 2010. Anatomy and controlling factors of a Late Cretaceous Aeolian sand sheet: The Marília and the Adamantina formations, NW Bauru Basin, Brazil. Sedimentary Geology, 226, 71-93.

Basilici, G., Dal' Bo, P. F., Oliveira, E. F., 2016a. Distribution of palaeosols and deposits in the temporal evolution of a semiarid fluvial distributary system (Bauru Group, Upper Cretaceous, SE Brazil). Sedimentary Geology, 341, 245-264.

Basilici, G., Fiorelli, L.E., Dal' Bo, P. F., 2016b. Comment on "Evolution and palaeoenvironment of the Bauru Basin (Upper Cretaceous, Brazil)" by Luiz Alberto Fernandes and Claudia Maria Magalhaes Ribeiro. Journal of South American Earth Sciences, 1-5. http://dx.doi.org/10.1016/j.jsames.2016.06.015.

Beerbower, J.R., 1964. Cyclothems and cyclic depositional mechanisms in alluvial plain sedimentation. In: Merriam, D.F., (Ed.), Symposium on Cyclic Sedimentation. Kansas Geological Survey Bulletin, 169.2.1.6., pp. 31-42.

Bridge, J.S., Leeder, M.R., 1979. A simulation model of alluvial stratigraphy. Sedimentology, 26, 617-644.

Bridge, J.S., 2006. Fluvial facies models: Recent developments. In: Posamentier, H.W., Walker, R.G., (Eds.), Facies Models Revisited. Society for Sedimentary Geology Special Publication, 84, pp. 85-170.

Cain, S.A., Mountney, N.P., 2009. Spatial and temporal evolution of a terminal fluvial fan system: the Permian Organ Rock Formation, South-east Utah, USA. Sedimentology, 56, 1774-1800.

Colombera, L., Mountney, N.P., McCaffrey, W.D., 2012. A Relational Database for the Digitization of Fluvial Architecture: Concepts and Example Applications. Petroleum Geoscience, 18, 129-140.

Colombera, L., Mountney, N.P., McCaffrey, W.D., 2013. A quantitative approach to fluvial facies models: methods and example results. Sedimentology, 60, 1526-1558.

Catt, J.A., 1990. Paleopedology Manual. Quaternary International, 6, 95.

Chakraborty, C., Bose, P.K., 1992. Ripple/dune to upper stage plane bed transition: some observations from the ancient record. Geological Journal, 27, 349-359.

Chumakov N.M., 1995. Climatic zones in the middle of the Cretaceous Period. Stratigraphy and Geological Correlation, 3, 3-14.

Collinson J, Mountney N.P., Thompson D, 2006. Sedimentary Structures. (Third Edition). Terra Publishing, pp. 292.

Cooke, R.U., Warren, A., Goudie, A.S., 1993. Desert Geomorphology. University College London Press, London, pp. 526.

Costa, J.E., 1988. Rheologic, geomorphic and sedimentologic differentiation of water floods, hyperconcentrated flows and debris flows. In: Baker, V.R., Kochel, R.C., Patton, P.C., (Eds.), Flood Geomorphology. John Wiley & Sons, Inc., Chichester, pp. 113-122.

Coutinho, J.M.V., Coimbra, A.M., Brandt Neto, M., Rocha, G.A., 1982. Lavas alcalinas analcimíticas associadas ao Grupo Bauru (Kb) no Estado de São Paulo, Brasil. In: Congresso Latinoamericano de Geologia, 5(2), pp. 185-196.

CPRM - Geological Survey of Brazil, 2004. Carta Geológica do Brasil ao Milionésimo, Folhas SE22 (Goiânia), SE23 (Belo Horizonte), SF22 (Paranapanema). Secretaria de Minas e Metalurgia e Ministério de Minas e Energia, Brasília.

Dal' Bó, P.F.F., Basilici, G., Angelica, R.S., Ladeira, F.S.B., 2009. Paleoclimatic interpretations from pedogenic calcretes in a Maastrichtian semiarid eolian sand-sheet palaeoenvironment: Marília Formation (Bauru Basin, southeastern Brazil). Cretaceous Research, 30, 659-675.

Dal' Bó, P.F.F., Basilici, G., Angélica, R.S., 2010. Factors of palaeosol formation in a Late Cretaceous eolian sand sheet paleoenvironment, Marília Formation, southeastern Brazil. Palaeogeography, Palaeoclimatology, Palaeoecology, 292, 349-365.

Dias-Brito, D., Musacchio, E.A., Castro, J.C., Maranhão, M.S.A.S., Suárez, J.M., Rodrigues, R., 2001. Grupo Bauru: uma unidade continental do Cretáceo do Brasil – Concepções baseadas em dados micropaleontológicos, isotópicos e estratigráficos. Revue Paléobiologie, Genebra, 2, 195-304.

Fenwick, I., 1985. Paleosols: problems of recognition and interpretation. In: Boardman, J., (Ed.), Soils and Quaternary Landscape Evolution. Wiley, Chichester, pp. 3-21.

Fielding, C.R., Alexander, J., McDonald, R., 1999. Sedimentary facies from GPR surveys of the modern, upper Burdekin River of north Queensland, Australia: Consequences of extreme discharge fluctuations. In: Smith, N.D., Rogers, J., (Eds.), Fluvial sedimentology VI. International Association of Sedimentologists Special Publication, 28, pp. 347-362.

Fielding, C.R., 2006. Upper flow regime sheets, lenses and scour fills: Extending the range of architectural elements for fluvial sediment bodies. Sedimentary Geology, 190, 227-240.

Fielding, C.R., Allen, J.P., Alexander, J., Gibling, M.R., 2009. Facies model for fluvial systems in the seasonal tropics and subtropics. Geology, 37, 623-626.

Graf, W.L., 1988. Fluvial Processes in Dryland Rivers. Springer-Verlag, Berlin, pp. 346.

Harms, J.C., Southard, J.B. and Walker, R.G., 1982. Structures and sequences in clastic rocks. Society of Economic Paleontologists and Mineralogists Short Course, No. 9.

Holbrook, J.M., Willis, B.J., Bhattacharya, J., 2003. The Evolution of Allocyclicity and Autocyclicity as Sedimentary Concepts. American Association of Petroleum Geologists Annual Meeting, Salt Lake City, Utah.

Hubert, J.F., Hyde, M.G., 1982. Sheet-flow deposits of graded beds and mudstones on an alluvial sandflat-playa system: Upper Triassic Blomidon redbeds, St Mary's Bay, Nova Scotia. Sedimentology, 29, 457-474.

Jones, L.S., Schumm, S.A., 1999. Causes of avulsion: an overview. In: Smith, N.D., Rogers, J., (Eds.), Fluvial Sedimentology VI. Special Publication, International Association of Sedimentologists, 28, pp. 171-178.

Jones, C.M., 1977. The effects of varying discharge regimes on bedform sedimentary structures in modern rivers. Geology, 5, 567-570.

Jopling, A.V., Walker, R.G., 1968. Morphology and origin of ripples-drift cross-lamination, with examples from the Pleistocene of Massachusetts. Journal of Sedimentary Petrology, 38, 971-984.

Jopling, A.V., 1965. Hydraulic factors and shape of laminae. Journal of Sedimentary Petrology, 35, 777-791.

Kraus, M.J., 1996. Avulsion deposits in Lower Eocene alluvial rocks, Bighorn Basin, Wyoming. Journal of Sedimentary Research, 66(2), 354-363.
Kraus, M.J., 1999. Paleosols in clastic sedimentary rocks: their geologic applications. Earth-Science Reviews, 47, 41-70.
Kraus, M.J., and Gwinn, B.M., 1997. Controls on the development of early Eocene avulsion deposits and floodplain paleosols, Willwood Formation, Bighorn Basin. Sedimentary Geology, 114, 33-54.
Kraus, M.J. and Wells, T.M., 1999. Recognizing avulsion deposits in the ancient stratigraphical record. Special Publication, International Association of Sedimentologists, 28, 251-268.
Leeder, M.R., 1978. A quantitative stratigraphic model for alluvium with special reference to channel deposit density and interconnectedness. In: Miall, A.D., (Ed.), Fluvial Sedimentology. Canadian Society of Petroleum Geologists, Memoir 5, pp. 587-596.
Lunt, I.A., Bridge, J.S., Tye, R.S., 2004. Development of a 3-D depositional model of a braided-river gravels and sands to improve aquifer characterization. Society for Sedimentary Geology Special Publication, 80, 139-169.
Maizels, J., 1990. Long-term paleochannel evolution during episodic growth of an exhumed Plio-Pleistocene alluvial fan, Oman. In: Rachocki, A.H., Church, M., (Eds.), Alluvial fans: A Field Approach: Chichester, U.K.. John Wiley & Sons Ltd., pp. 271-304.
Makaske, B., 2001. Anastomosing rivers: a review of their classification, origin and sedimentary products. Earth-Science Reviews, 53, 149-196.
Makaske, B., Smith, D.G., Berendsen, H.J.A., 2002. Avulsions, channel evolution and floodplain sedimentation rates of the anastomosing upper Columbia River, British Columbia, Canada. Sedimentology, 49, 1049-1071.
Martinelli, A.G., Bogan, S., Agnolin, F.L., Ribeiro, L.C.B., Cavellani, C.L., Ferraz, M.L.F., Teixeira, V.P.A, 2013. First fossil record of amiid fishes (Halecomorphi, Amiiformes, Amiidae) from the Late Cretaceous of Uberaba, Minas Gerais State, Brazil. Alcheringa: An Australasian Journal of Palaeontology, 37, 105-113.
Martinelli, A.G., Teixeira, V.P.A., 2015. The Late Cretaceous vertebrate record from the Bauru Group in the Triângulo Mineiro, southeastern Brazil. Boletín Geológico y Minero, 126(1), 129-158.
McKie, T., 2011. Architecture and behaviour of dryland fluvial reservoirs, Triassic Skagerrak Formation, central North Sea. In: Davidson, S.K., North, C.P., Leleu, S., (Eds.), From River to Rock Record: The Preservation of Fluvial Sediments and their Subsequent Interpretation. Society for Sedimentary Geology Special Publication, 97, pp. 189-214.
Meredith, K.T., Hollins, S.E., Hughes, C.E., Cendón, D.I., Chisari, R., Griffiths, A., Crawford, J., 2015. Evaporation and concentration gradients created by episodic river recharge in a semiarid zone aquifer: Insights from $Cl^-$, $\delta^{18}O$, $\delta^2H$ and $^3H$. Journal of Hydrology, 529, 1070-1078.
Miall, A.D., 1996. The geology of fluvial deposits: Sedimentary facies, basin analysis, and petroleum geology. Berlin, Springer, pp. 582.
Miall, A.D., 2006. The Geology of Fluvial Deposits: Sedimentary Facies, Basin Analysis and Petroleum Geology. Springer, Berlin, pp. 582.
Milani, E.J., Melo, J.H.G., Souza, P.A., Fernandes, L.A., França, A.B., 2007. Bacia do Paraná. Boletim de Geociências Petrobrás, 15(2), 265-287.
Nemec, W., Steel, R.J., 1984. Alluvial and coastal conglomerates: Their significant features and some comments on gravelly mass-flow deposits. In: Koster, E.H., Steel, R.J., (Eds.), Sedimentology of Gravels and Conglomerates. Canadian Society of Petroleum Geologists Memoir, 10, pp. 1-31.
Nesbitt, H.W., Young, G.M., 1982. Early Proterozoic climates and plate motions inferred from major element chemistry of lutites. Nature, 299, 715-717.

Nichols, G.J., Fisher, J.A., 2007. Processes, facies and architecture of distributive fluvial system deposits. Sedimentary Geology, 195, 75-90.

Novas, F.E., Carvalho, I.S., Ribeiro, L.C.B., Méndez, A.H., 2008. First abelisaurid bone remains from the Maastrichtian Marília Formation, Bauru Group, Brazil. Cretaceous Research, 29, 625-635.

Parkash, B., Awasthi, A.K., Gohain, K., 1983. Lithofacies of the Markanda terminal fan, Kurukshetra district, Haryana, India. In: Collinson, J.D., Lewin, J., (Eds.), Modern and Ancient Fluvial Systems. Special Publication of the International Association of Sedimentologists No. 6. Blackwell Scientific Publications, Oxford, pp. 337-344.

Plink-Björklund, P., 2015. Morphodynamics of rivers strongly affected by monsoon precipitation: Review of depositional style and forcing factors. Sedimentary Geology, 323, 110-147.

Reid, I., Frostick, L.E., 2011. Channel form, flows and sediments of endogenous ephemeral rivers in deserts. In: Thomas, D.S.G., (Ed.), Arid Zone Geomorphology: Process, Form and Change in Drylands (Third Edition). John Wiley & Sons, Chichester, pp. 301-332.

Retallack, G.J., 1988. Field recognition of paleosols. In: Reinhardt, J., Sigleo, W.R., (Eds.), Paleosol and Weathering Through Geologic Time: Techniques and Applications. Geological Society of America, Special Paper, pp. 216, 1-20.

Røe, S.L., 1987. Cross-strata bedforms of probable transitional dune to upper-stage plane-bed origin from a Late Precambrian fluvial sandstone, northern Norway. Sedimentology, 34, 89-101.

Sanz-Montero, M.E., Cabestrero, O., Rodríguez-Aranda, J.P., 2014. Sedimentary effects of flood-producing windstorms in playa lakes and their role in the movement of large rocks. Earth Surface Processes and Landforms, 40, 864-875.

Schick, A.P., 1993. Geomorphology in Israel. In: Walker, H.J., Grabau, W.E., (Eds.), The Evolution of Geomorphology. Wiley, Chichester, pp. 231-237.

Slingerland, R., Smith, N.D., 2004. River avulsions and their deposits. Annual Review of Earth and Planetary Sciences, 32, 257-285.

Soares, P.C., Landim, P.M.B., Fúlvaro V.J., Sobreiro Neto, A.F., 1980. Ensaio de caracterização do Cretáceo no Estado de São Paulo: Grupo Bauru. Revista Brasileira de Geociências, 10(3), 177-185.

Stouthamer, E., Berendsen, H.J.A., 2007. Avulsion: the relative roles of autogenic and allogenic processes. Sedimentary Geology, 198, 309-325.

Thornes, J.B., 1994. Catchment and channel hydrology. In: Abrahams, A.D., Parsons, A.J., (Eds.), Geomorphology of Desert Environments. Chapman & Hall, London, pp. 257-287.

Tooth, S., 1999. Downstream changes in floodplain character on the Northern Plains of arid central Australia. In: Smith, N.D., Rogers, J., (Eds.), Fluvial Sedimentology VI. International Association of Sedimentologists, Special Publication 28, Blackwell Scientific Publications, Oxford, pp. 93-112.

Tooth, S., 2000. Process, form and change in dryland rivers: a review of recent research. Earth-Science Reviews, 51, 67-107.

Tooth, S., Nanson, G.C., 1995. The geomorphology of Australia's fluvial systems: retrospect, perspect and prospect. Progress in Physical Geography, 19, 35-60.

Törnqvist, T.E., Bridge, J.S., 2002. Spatial variation of overbank aggradation rate and its influence on avulsion frequency. Sedimentology, 49, 891-905.

Tunbridge, I.P., 1984. Facies model for a sandy ephemeral stream and clay playa complex: the Middle Devonian Trentishoe Formation and North Devon, UK. Sedimentology, 31, 697-715.

Weissmann, G.S., Hartley, A.J., Nichols, G.J., Scuderi, L.A., Olson, M., Buehler, H., Banteah, R., 2010. Fluvial form in modern continental sedimentary basins: distributive fluvial systems. Geology, 38, 39-42.